SANDIA REPORT
SAND2014-1961
Unlimited Release
Printed March 2014

Analysis report for WIPP colloid model constraints and performance assessment parameters

Paul E. Mariner and David C. Sassani

Prepared by
Sandia National Laboratories
PO Box 5800
Albuquerque, New Mexico 87185-0747

Sandia National Laboratories is a multi-program laboratory managed and operated by Sandia Corporation, a wholly owned subsidiary of Lockheed Martin Corporation, for the U.S. Department of Energy's National Nuclear Security Administration under contract DE-AC04-94AL85000.

Approved for public release; further dissemination unlimited.

Sandia National Laboratories

Issued by Sandia National Laboratories, operated for the United States Department of Energy by Sandia Corporation.

NOTICE: This report was prepared as an account of work sponsored by an agency of the United States Government. Neither the United States Government, nor any agency thereof, nor any of their employees, nor any of their contractors, subcontractors, or their employees, make any warranty, express or implied, or assume any legal liability or responsibility for the accuracy, completeness, or usefulness of any information, apparatus, product, or process disclosed, or represent that its use would not infringe privately owned rights. Reference herein to any specific commercial product, process, or service by trade name, trademark, manufacturer, or otherwise, does not necessarily constitute or imply its endorsement, recommendation, or favoring by the United States Government, any agency thereof, or any of their contractors or subcontractors. The views and opinions expressed herein do not necessarily state or reflect those of the United States Government, any agency thereof, or any of their contractors.

Printed in the United States of America. This report has been reproduced directly from the best available copy.

Available to DOE and DOE contractors from
U.S. Department of Energy
Office of Scientific and Technical Information
P.O. Box 62
Oak Ridge, TN 37831

Telephone: (865) 576-8401
Facsimile: (865) 576-5728
E-Mail: reports@adonis.osti.gov
Online ordering: http://www.osti.gov/bridge

Available to the public from
U.S. Department of Commerce
National Technical Information Service
5285 Port Royal Rd.
Springfield, VA 22161

Telephone: (800) 553-6847
Facsimile: (703) 605-6900
E-Mail: orders@ntis.fedworld.gov
Online order: http://www.ntis.gov/help/ordermethods.asp?loc=7-4-0#online

SAND2014-1961
Unlimited Release
Printed March 2014

Analysis report for WIPP colloid model constraints and performance assessment parameters

Paul E. Mariner and David C. Sassani
Advanced Nuclear Energy Programs
Sandia National Laboratories
P.O. Box 5800
Albuquerque, New Mexico 87185-MS-0747

ABSTRACT

An analysis of the Waste Isolation Pilot Plant (WIPP) colloid model constraints and parameter values was performed. The focus of this work was primarily on intrinsic colloids, mineral fragment colloids, and humic substance colloids, with a lesser focus on microbial colloids. Comments by the US Environmental Protection Agency (EPA) concerning intrinsic Th(IV) colloids and Mg-Cl-OH mineral fragment colloids were addressed in detail, assumptions and data used to constrain colloid model calculations were evaluated, and inconsistencies between data and model parameter values were identified. This work resulted in a list of specific conclusions regarding model integrity, model conservatism, and opportunities for improvement related to each of the four colloid types included in the WIPP performance assessment.

CONTENTS

Abstract 3
Contents 5
Figures 6
Tables 7
Nomenclature 8
1 Introduction 9
2 Colloids 11
2.1 Types of Colloids 11
2.2 Colloid Stability 11
3 WIPP Environment 13
4 WIPP Colloid Model 15
4.1 Conceptual Model 15
4.2 WIPP Colloid Model Equations and Parameters 16
4.2.1 Mineral fragment colloids 18
4.2.2 Intrinsic colloids 19
4.2.3 Humic substance colloids 20
4.2.4 Microbial colloids 22
4.3 WIPP Colloid Model Results 23
5 WIPP Colloid Parameter Analyses 25
5.1 Mineral Fragment Colloids 25
5.1.1 EPA Comments 25
5.1.2 Current PA Representation 25
5.1.3 Literature Review 25
5.1.4 Analysis 27
5.1.5 Conclusions 31
5.2 Intrinsic Colloids 31
5.2.1 EPA Comments 31
5.2.2 Current PA Representation 32
5.2.3 Literature Review 32
5.2.4 Analysis 33
5.2.5 Conclusions 36
5.3 Humic Substance Colloids 37
5.3.1 EPA Comments 37
5.3.2 Current PA Representation 37
5.3.3 Literature Review 38
5.3.4 Analysis 38
5.3.5 Conclusions 46
5.4 Microbial Colloids 47
5.4.1 EPA Comments 47

5.4.2 Current PA Representation 47
5.4.3 Literature Review 47
5.4.4 Analysis 48
5.4.5 Conclusions 51

6 Summary 53

7 References 55

Distribution 60

FIGURES

Figure 4-1. Solubility of Pu(IV)-polymer in NaCl media as a function of pcH (DOE 1996, Figure SOTERM-8). 20

Figure 4-2. CCA results for direct brine release to the Culebra in terms of source constituents (Helton et al. 1998, Figure 11.1.1). 24

Figure 5-1.Colloid concentrations from natural systems and simple salt solutions as function of ionic strength as compiled by Serco (Alexander et al. 2011, Figure 5.1). 29

Figure 5-2. Humic acid concentration over time for different liquid:solid ratios for both 95% GWB and 95% ERDA-6 (graphic from Wall and Mathews (2003)). 39

Figure 5-3. Histogram of measured $[AnHS]/[An]$ ratios for Th(IV) in seawater (calculated from Table 4 of Baskaran et al. 1992). 45

Figure 5-4. Microbial actinide concentrations calculated from baseline CRA-2014 $[An]$ values, Reed et al. (2013a, Table 6-2) oxidation-state-specific (ox) parameters for archaea, and Reed et al. (2013a, Table 6-3) element-specific (elem) parameters for archaea compared to values calculated from CRA-2009 PROPMIC and CAPMIC. ..50

Figure 5-5. Microbial actinide concentrations calculated from baseline CRA-2014 $[An]$ values, Reed et al. (2013a, Table 6-2) oxidation-state-specific (ox) parameters for bacteria, and Reed et al. (2013a, Table 6-3) element-specific (elem) parameters for bacteria compared to values calculated from CRA-2009 PROPMIC and CAPMIC. 50

TABLES

Table 3-1. Predicted compositions of GWB and ERDA-6 in the minimum volume (1 × Min) and five times the minimum volume (5 × Min) of brine required for a direct brine release (DBR) from the repository (Brush and Domski 2013b).....14

Table 4-1. WIPP colloid model parameter summary and description (DOE 1996, Appendix SOTERM, Table SOTERM-8).....17

Table 4-2. WIPP colloid parameter values used in the CCA (DOE 1996, Appendix SOTERM, Table SOTERM-14).....18

Table 4-3. Calculated values of humic-bound actinide concentrations $[\mathbf{AnHS}]$ and proportionality constants (i.e., PHUMSIM and PHUMCIM) for U(VI), Np(V), and Am(III). Inputs from Papenguth (1996, Tables 1a, 1b, and 3).....22

Table 5-1. Concentrations of intrinsic colloids measured in WIPP brines in long-term experiments at anticipated pcH values.....33

Table 5-2. Average pH and 60-day humic acid concentration in presence and absence of MgO in Wall and Mathews (2005) study.....39

Table 5-3. Calculated values of humic-bound actinide concentrations $[\mathbf{AnHS}]$ and $[\mathbf{AnHS}]/[\mathbf{An}]$ using CRA-2014 PA solubility (estimated using minimum brine volume) combined with constants from Papenguth (1996, Tables 1a, 1b, and 3).....42

Table 5-4. Calculated values of humic-bound actinide concentrations $[\mathbf{AnHS}]$ and $[\mathbf{AnHS}]/[\mathbf{An}]$ using halved values for $\beta_{1:An}$ and $[\mathbf{HS_{tot}}]$ and a doubled value for $\beta_{1:CaMg}$ compared to Table 4-3.....43

Table 5-5. Calculated values of humic-bound U(VI) concentrations $[\mathbf{AnHS}]$ and $[\mathbf{AnHS}]/[\mathbf{An}]$ using the U(VI) complexation constants of Labonne-Wall et al. (1999).....44

Table 5-6. Baseline humic-bound actinide concentrations consistent with CRA-2014 PA actinide solubilities.....46

Table 5-7. PROPMIC and CAPMIC values used in the CRA-2014 PA (Roselle 2013b).....47

NOMENCLATURE

An	Actinide
AnHS	Actinide-humic site complex
AnMIC	Actinide-microbial site complex
CAPHUM	Maximum concentration of actinide associated with mobile humic colloids
CAPMIC	Maximum concentration of actinide associated with mobile microbes
CCA	Compliance Certification Application
CFR	Code of Federal Regulations
CONCINT	Concentration of actinide associated with mobile intrinsic actinide colloids
CONCMIN	Concentration of actinide associated with mobile mineral fragment colloids
CRA	Compliance Recertification Application
DLVO	A particle interaction theory based on the works of Derjaguin and Landau (1941) and and Verwey and Overbeek (1948)
DOE	U.S. Department of Energy
EPA	U.S. Environmental Protection Agency
ERDA-6	Energy Research and Develop Administration WIPP Well 6
GWB	Generic Weep Brine
HLW	High-level radioactive waste
LANL	Los Alamos National Laboratory
LLNL	Lawrence Livermore National Laboratory
MgO	Magnesium oxide
NM	New Mexico
PA	Performance Assessment
PABC	Performance Assessment Baseline Calculation
pcH	Negative log of the calculated molar concentration of hydrogen ion
pH	Negative log of the hydrogen ion activity
PHUMCIM	Proportionality constant for concentration of actinides associated with mobile humic colloids in Castile brine
PHUMSIM	Proportionality constant for concentration of actinides associated with mobile humic colloids in Salado brine
PROPMIC	Proportionality constant for concentration of actinides associated with mobile microbes
SNL	Sandia National Laboratories
TRU	Transuranic (waste)
WIPP	Waste Isolation Pilot Plant

1 INTRODUCTION

The Waste Isolation Pilot Plant (WIPP) is a deep geologic repository developed by the U.S. Department of Energy (DOE) for the disposal of transuranic (TRU) radioactive waste. The repository is located within the bedded salts of the Permian Salado Formation, consisting mainly of rock salt with thin interbedded layers of anhydrite and polyhalite. Containment of TRU waste at the WIPP is regulated by the U.S. Environmental Protection Agency (EPA) according to requirements set forth in Title 40 of the Code of Federal Regulations (CFR), Part 191. The DOE demonstrates compliance with containment requirements by means of performance assessment (PA). WIPP PA calculations are used to estimate the probability and consequence of actinide releases from the repository to the accessible environment for a regulatory period of 10,000 years after facility closure.

The WIPP PA includes modeling the consequences of inadvertent human intrusions resulting from future exploratory drilling. Such intrusions could lead to a postulated release of actinides to the accessible environment before the end of the 10,000 year regulatory period. To accomplish this, the DOE has examined different drilling scenarios, which involve the penetration of the repository by one or more drill holes. Some of the scenarios also involve the possibility of the penetration of a pressurized brine reservoir in the Castile Formation beneath the Salado. In the WIPP PA, these intrusion scenarios lead to actinide release at the surface or in some cases to the Culebra aquifer approximately 400 m above the repository. The concentrations of actinides in the simulated releases are a function of actinide oxidation state, aqueous solubility, and colloid enhancement factors. Depending on the actinide, WIPP PA releases can be significantly enhanced by colloids (Section 4.3).

The WIPP is required to be recertified by the EPA every five years. In 2010, an EPA review (EPA 2010) of the 2009 WIPP recertification application, CRA-2009 (DOE 2009), resulted in requests by the EPA that the DOE, prior to the next recertification (CRA-2014), re-evaluate thorium intrinsic colloids and Mg-Cl-OH mineral fragment colloids under WIPP-relevant conditions. In response, the DOE initiated a concerted effort to reanalyze the technical bases for the parameters in all WIPP PA colloid models. This analysis report summarizes the reanalysis.

More data are available in the literature for more detailed assessment of colloid stability and actinide transport behavior than existed during the WIPP colloid model development effort for the Compliance Certification Application (CCA) (DOE 1996). Conceptual models have been developed for a variety of colloid types for evaluating performance of a repository system at Yucca Mountain (Buck and Sassani 2007). Together with the current expected conditions for the WIPP repository system and the additional WIPP testing data being collected, the availability of new data from colloids studies allows for a productive re-evaluation of the uncertainty and level of conservatism within the WIPP colloids models. Such synthesis provides a context within which to evaluate changes to parameter values for the WIPP colloid models, either for use in sensitivity analyses to delineate and quantify degrees of conservatism, or for use directly in updated performance assessments.

The present analysis is a Programmatic Decision analysis per NP 9-1. This analysis report is completed under the Analysis Plan for Evaluating Constraints on Colloid Parameters in the WIPP Repository, AP 152, Rev. 0 (Sassani 2011). Because of changes in detailed scope of specific coverage of the colloid types, the deviations from the planned work are that (a) a single analysis report is written to cover the analyses outlined in Sassani (2011); (b) the primary focus of the analyses is on intrinsic colloids, mineral fragment colloids, and humic substance colloids, with lesser analysis of microbial colloids, and (c) additional relevant laboratory work performed at LANL is analyzed.

2 COLLOIDS

Colloids are important to PA because they can be responsible for significant fractions of the mobile concentrations of actinides. Colloids are composed of minute particles of phases (~ 1 nm to 1 μm (Kim 1994)) that are less stable than macroscopic particles of the same phase because of high surface free energy at such small particle diameters. Even though the particles are metastable, they may persist in systems because of kinetic inhibitions to achieve equilibrium especially in conjunction with proximity to the unstable generating source of the metastable colloids. Both solution pH and ionic strength (actually cation content) of the solution are the major influences that cause colloids to transition from "stable" (i.e., persisting in solution without changing in concentration or size) to "unstable" (i.e., aggregating and flocculating) such that the concentration in the aqueous phase decreases by orders of magnitude.

2.1 Types of Colloids

Groundwater colloids are found in a variety of forms. One form is intrinsic (or true) colloids. Intrinsic colloids are macromolecules of actinides in which the actinides are a structural part of the colloid atomic makeup. These colloids form in the nanometer range and may mature/grow into larger particles. When immature they are hydrophilic but as they grow, they become hydrophobic, meaning that the stability of their suspension becomes dependent on the electrostatic interactions within the solution. When mature, they can act as mineral fragment colloids, allowing for other dissolved constituents to attach to their surface.

Mineral fragment colloids, also known as pseudo-colloids, are hydrophobic hard sphere particles whose suspensions are stabilized/destabilized by electrostatic forces between their surfaces and the solution. A variety of minerals/substances either crystalline or amorphous may form mineral fragment colloids; they are thermodynamically metastable versions of their larger or more crystalline counterpart minerals. Mineral fragment colloids provide sorptive substrates for transporting actinides and can incorporate actinides via coprecipitation mechanisms.

Colloids may also be organic. Humic substances colloids are hydrophilic humic substance molecules (up to 100,000 atomic mass units) stabilized in solution by solvation forces. These colloids provide sorptive substrates for actinides. Microbial colloids are comparatively large particles (up to the limit of one micron) and are stabilized by hydrophilic coatings on their surfaces. Microbes provide sorptive substrates for actinides and can also bioaccumulate actinides. Each of these types of colloids is included in the WIPP PA colloid model (Section 4.2).

2.2 Colloid Stability

The solution composition (particularly the cation concentrations, as affected by ionic strength and the solution pH) is a key factor in the rate of colloid aggregation and the stability of colloids. At higher ionic strength and/or pH near the pH of net neutral charge for colloid particles, the rates of aggregation and flocculation tend to increase, reducing the stability of colloids. Considerations of whether colloids may be relevant to a system include identifying the colloid sources, determining whether these sources are local or distal, and evaluating the stability of the colloids given the aqueous chemical conditions and colloid surface properties.

Colloids have a high degree of stability when aggregation rates are low. This condition occurs when repulsive forces of electrostatic double layers are strong enough to prevent colloid particles from coming close enough together to bind together by attractive van der Waals forces. Because the chemistry of the water affects the charge and thickness of the double layer, it directly affects the magnitude of the energy barrier that inhibits close particle-particle encounters and hence aggregation. The energy barrier can be approximated by DLVO theory by summing van der Waals forces and electric double layer forces as a

function of inter-particle distance (Derjaguin and Landau 1941; Verwey and Overbeek 1948). Such calculations show that mineral fragment colloids have energy barriers to aggregation that are a function of pH and can decrease to zero at ionic strengths rising only into the tens of mM range (e.g., Hu et al. 2010; Abdel-Fattah et al. 2013). In the case of Pu(IV), its intrinsic colloids can readily aggregate with natural groundwater colloids to form highly mobile pseudocolloids (Abdel-Fattah et al. 2013). Data also indicate that the presence of humic acids can increase the stability of mineral fragment colloids by (1) increasing the electrostatic repulsion between particles and (2) presenting steric barriers to close encounters between mineral fragment colloid surfaces (Borgnino 2013).

Depending on the rates of generation and flocculation, colloids that are highly unstable may persist for long periods of time. Proximal sources of colloids may have rates of production that maintain a state far from equilibrium. This can be the case for waste forms and engineered materials that are actively altering within the local chemistry. Because colloid formation is a path-dependent process, evaluations of suspended colloid concentrations must consider the paths involved.

Traexler et al. (2004) and Zhao and Steward (1997) extensively reviewed colloid formation from nuclear waste forms and concluded that all waste forms may form colloids during alteration. The models developed for high level waste disposal at Yucca Mountain (Buck and Sassani 2007) focused on both the colloid-formation processes and colloid stability within the waste package and engineered barrier system environments. That work provides a detailed discussion of the chemical environment controls on colloid stability and a rigorous quantitative model of colloid stability. That model is supported by observations for natural mineral colloids from a variety of systems as discussed in Section 5.1.4.3. Although a number of the specific colloids (i.e., waste form colloids) considered for the Yucca Mountain performance assessment are not relevant to the WIPP source term, the general discussion of colloid sources and the specific considerations of colloid stability are directly relevant.

3 WIPP ENVIRONMENT

The nature of the environment within the WIPP repository following closure will, to a large extent, control the stability and abundance of colloids. As discussed in Section 2.2, the stability and abundance of colloids are strongly affected by groundwater composition (e.g., ionic strength and pH). They are also strongly affected by the relative rates of colloid generation (e.g., from metal corrosion), aggregation, and flocculation.

The compositions of groundwater in the Salado and Castile formations are represented in the WIPP PA respectively by GWB (Generic Weep Brine) and ERDA-6 (Energy Research and Develop Administration WIPP Well 6). The compositions of these brines after equilibration with halite (NaCl), anhydrite ($CaSO_4$), hydromagnesite ($Mg_5(CO_3)_4(OH)_2{\cdot}4H_2O$), and brucite ($Mg(OH)_2$) are shown in Table 3-1 for the minimum volume of brine required for a direct brine release (DBR) from the repository and for five times the minimum volume (Brush and Domski 2013b).

Metal corrosion within the WIPP repository may generate mineral fragment colloids and may serve to maintain reducing conditions. The corrosion behavior of these metals, specifically the kinetics of the corrosion reaction, will be controlled by the availability of H_2O at the metal surface, as well as the internal environment within the repository. If the corrosion rate is rapid relative to the rate of aggregation and flocculation, enhanced concentrations of colloids may be sustained in the vicinity of the corrosion reactions.

The predominant metals within the repository will be iron (Fe) in the form of low-carbon steel and chemical-grade lead (Pb). These metals are present within the waste itself, as well as the containers used to hold the waste during emplacement. In addition to Fe and Pb, the waste disposed within WIPP contains significant quantities of cellulosic, plastic and rubber materials. With time, microbial activity may consume some portion of these organic materials, resulting in generation of significant quantities of carbon dioxide (CO_2), hydrogen sulfide (H_2S), hydrogen (H_2), nitrogen (N_2) and methane (CH_4).

Corrosion of steel and biodegradation of organic materials have been identified as major gas generation processes in the repository (Brush 1995). Gas production will affect room closure and chemistry (Butcher 1990; Brush 1990). Wang and Brush (1996) provided estimates of gas generation parameters for the long-term WIPP performance assessment based on experimental work of Telander and Westerman (1997). These rates have been revised over the years, most recently by Roselle (2013a). These parameters included steel corrosion rates under inundated and humid conditions, the stoichiometric factors of gas generation reactions, and the probability of occurrence of organic material biodegradation. Biodegradation supports microbial communities, and, with the ambient populations of microbes in the WIPP system, contributes directly to microbial colloids in the WIPP source-term.

Table 3-1. Predicted compositions of GWB and ERDA-6 in the minimum volume (1 × Min) and five times the minimum volume (5 × Min) of brine required for a direct brine release (DBR) from the repository (Brush and Domski 2013b)

Element or Property	Units	GWB (1 × Min[a])	GWB (5 × Min)	ERDA-6 (1 × Min)	ERDA-6 (5 × Min)
B(III) (aq)	M	0.186	0.186	0.0623	0.0624
Na(I) (aq)	M	4.77	4.78	5.30	5.33
Mg(II) (aq)	M	0.330	0.313	0.136	0.111
K(I) (aq)	M	0.550	0.549	0.0960	0.0960
Ca(II) (aq)	M	0.0111	0.0113	0.0116	0.0119
S(VI) (aq)	M	0.216	0.205	0.182	0.171
Cl(-I) (aq)	M	5.36	5.39	5.24	5.26
Br(-I) (aq)	M	0.0313	0.0313	0.0109	0.0109
CO_2 fugacity	atm	3.14×10^{-6}	3.14×10^{-6}	3.14×10^{-6}	3.14×10^{-6}
Ionic strength	M	6.44	6.41	5.99	5.94
pcH[b]	-log(M)	9.54	9.54	9.69	9.72
Total inorganic carbon	M	3.79×10^{-4}	3.80×10^{-4}	4.55×10^{-4}	4.75×10^{-4}

[a] Min = minimum brine volume for a DBR from the repository (17,400 m^3)

[b] Negative log of the hydrogen ion concentration (M)

4 WIPP COLLOID MODEL

Colloids are included in the WIPP PA because colloids can increase the mobility of actinides (e.g., Abdel-Fattah et al. 2013) and therefore can increase the quantity of actinides released to the accessible environment. The colloid model is implemented in the WIPP PA to guard against the possibility of underestimating the release of actinides to the biosphere. For scenarios in which actinides must migrate through the Salado or Culebra formations to reach the biosphere, colloids have the additional potential effect of enhancing actinide transport.

The WIPP colloid model was developed for the CCA (DOE 1996, Appendix SOTERM, Section SOTERM.6.3), repeated in the CRA-2004 (DOE 2004, Appendix PA, Attachment SOTERM, Section SOTERM-6.0), and summarized in the CRA-2009 (DOE 2009, Appendix SOTERM-2009, Sections SOTERM-4.7 and SOTERM-5.0). This model has changed little from its original form as documented in the CCA. Section 4.1 summarizes the conceptual model, Section 4.2 summarizes the model equations and parameters, and Section 4.3 summarizes past results of the model.

4.1 Conceptual Model

There are four types of colloids in the WIPP colloid model: intrinsic, mineral fragments, humic substances, and microbes. Each of these colloid types is defined and described in Section 2.1. In the conceptual model, inorganic colloids (intrinsic and mineral fragments) may form by nucleation when the aqueous phase becomes supersaturated with respect to the mineral phase or when mixed metal ions undergo hydrolysis reactions (Kim 1992). Intrinsic colloids form readily under a variety of groundwater conditions (e.g., Johnson and Toth 1978; Nitsche et al. 1992; Nitsche et al. 1994; Reed et al. 2013a). In addition to nucleation, natural mineral fragment particles may be released from the host rock due to changes in chemistry or physical disruption. Mineral fragment colloids may also be introduced by the corrosion of the waste materials and solid materials within the waste, by the degradation of cement, and by the use of drilling mud. Potential sources of organic colloids (humic substances and microbes) include organic and soil-bearing wastes disposed in the repository as well as naturally-occurring organic colloids in the groundwaters of the Salado, Castile, or Culebra formations. Humic substances may additionally be generated by the degradation of insoluble organic wastes. Due to the introduction of a variety of new materials, natural microbial populations are likely to increase. The WIPP PA model was developed to account for the presence, introduction, and generation of each of these potential colloid sources (DOE 1996, Section SOTERM.6.3).

Each colloid type in the conceptual colloid model has a different primary mechanism for incorporating actinides. Intrinsic colloids are largely composed of a single actinide and are not considered to appreciably sorb other actinides. Mineral fragment colloids incorporate actinides primarily by sorption or surface co-precipitation. Humic substance colloids incorporate actinides primarily by complexation with their carboxylic and hydroxyl functional groups. Microbial colloids may incorporate actinides by both surface association and intracellular bioaccumulation. Each of these mechanisms is conceptually considered in the quantitative constraints developed for the colloid model (Section 4.2).

In the WIPP PA, fluid movement is an important mechanism for the transport and release of actinides to the biosphere. Colloids may enhance this release by increasing the fluid concentrations of actinides that may be transported to the surface or to the Culebra. Colloids may also increase the velocity of the transport of actinides through the Culebra. For these reasons, and to account for potential colloid facilitation of actinide release, the conceptual WIPP colloid model is designed to be conservative and includes the following conservative assumptions (DOE 1996, SOTERM.6.3):

- Colloids do not sorb to immobile porous media.

- Colloids remain in the mobile phase and are not immobilized by filtration.
- Each actinide fills the entire site capacity of mineral fragment colloids (provided sufficient actinide inventory).
- There is no competition among actinides for sorption sites on colloids.

To further minimize the likelihood of underestimating colloidal contributions to actinide mobility, the WIPP colloid model generally uses conservative values of the concentrations of colloids in the groundwater and in many cases conservative values of the amounts of actinides associated with these colloids. The model equations and parameter values for each colloid type are summarized in Section 4.2.

4.2 WIPP Colloid Model Equations and Parameters

In the WIPP PA, the source term contains both dissolved actinides constrained by solubility limits of actinide phases and actinides that are associated with colloids. The concentration of each actinide associated with each colloid type is determined individually and added to the dissolved actinide concentration to compute the total mobilized concentration of each actinide. For the inorganic colloids an absolute concentration of the colloid type is added to the dissolved source term. For organic colloids, proportionality constants and upper limits on capacity are used.

Table 4-1 lists and summarizes the WIPP colloid model parameters. These parameters are described mathematically in Sections 4.2.1 through 4.2.4 where the model equations for each colloid type are summarized. Based on these parameters, the mobile actinide concentrations in Castile and Salado brines are calculated as in Eq. 1 and 2 below, provided (1) sufficient actinide inventory and (2) microbial and humic substance colloid contributions do not exceed CAPMIC and CAPHUM, respectively:

$$MobileAnCastile = DissolvedAnCastile * (1 + \mathrm{PROPMIC} + \mathrm{PHUMCIM}) + \mathrm{CONCINT} + \mathrm{CONCMIN} \quad \text{(Eq. 1)}$$

$$MobileAnSalado = DissolvedAnSalado * (1 + \mathrm{PROPMIC} + \mathrm{PHUMSIM}) + \mathrm{CONCINT} + \mathrm{CONCMIN} \quad \text{(Eq. 2)}$$

The parameters $DissolvedAnSalado$ and $DissolvedAnCastile$ are often represented in this report as $[\mathrm{An}]$. When calculated microbial and/or humic colloid actinide concentrations exceed CAPMIC and/or CAPHUM, the microbial and/or humic contributions are limited to CAPMIC and/or CAPHUM, respectively.

The values of the colloid model parameters used in the CCA are listed in

Table 4-2. As of the CRA-2009 PA, three changes to these values were in effect, as indicated in Table SOTERM-22 of DOE (2009):

- CAPMIC for Am(III) was set to 1.0 M.
- CONCINT for Pu(III) was set to 1.0×10^{-9} M.
- CAPMIC for U(VI) was set to 0.0021 M.

The full set of parameter values is the subject of the analyses performed in Section 5. In addition, for the CRA-2014, new parameters for the microbial colloids are used based on recommendations by Reed et al. (2013a); these recommendations are addressed in Section 5.4.

Table 4-1. WIPP colloid model parameter summary and description (DOE 1996, Appendix SOTERM, Table SOTERM-8)

IDMTRL	IDPRAM	Brief Description of Parameter
Th, U, Np, Pu, Am	CONCMIN	concentration of actinide associated with mobile mineral fragment colloids
Th, U, Np, Pu, Am	CONCINT	concentration of actinide associated with mobile actinide intrinsic colloids
Th, U, Np, Pu, Am	PROPMIC	proportionality constant for concentration of actinides associated with mobile microbes.
PHUMOX3* PHUMOX4 PHUMOX5 PHUMOX6	PHUMCIM	proportionality constant for concentration of actinides associated with mobile humic colloids, in Castile brine, actinide solubilities are inorganic only (complexes with man-made organic ligands are not important), solubilities were calculated assuming equilibrium with Mg-bearing minerals (brucite and magnesite);
PHUMOX3* PHUMOX4 PHUMOX5 PHUMOX6	PHUMSIM	proportionality constant for concentration of actinides associated with mobile humic colloids, in Salado brine, actinide solubilities are inorganic only (complexes with man-made organic ligands are not important), solubilities were calculated assuming equilibrium with Mg-bearing minerals (brucite and magnesite).
Th, U, Np, Pu , Am	CAPMIC	maximum (cap) concentration of actinide associated with mobile microbes;
Th, U, Np, Pu, Am	CAPHUM	maximum (cap) concentration of actinide associated with mobile humic colloids.

* Proportionality constant for concentration of actinides associated with mobile humic substances, for PHUMOX3, for actinide elements with oxidation state 3 [that is, Pu(III) and Am(III)]; PHUMOX4, oxidation state 4 [that is, Th(IV), U(IV), Np(IV), and Pu(IV)]; PHUMOX5, oxidation state 5 [that is, Np(V)]; and PHUMOX6, oxidation state 6 [that is, U(VI)].

Table 4-2. WIPP colloid parameter values used in the CCA (DOE 1996, Appendix SOTERM, Table SOTERM-14)

	CONCMIN Concentration on Mineral Fragments[a]	CONCINT Concentration as Intrinsic Colloid[a]	PROPMIC Proportion Sorbed on Microbes[b]	CAPMIC Maximum Sorbed on Microbes[c]	Proportion Sorbed on Humics[b]		CAPHUM Maximum Sorbed on Humics[a]
					PHUMSIM Salado	PHUMCIM Castile	
Th(IV)	2.6×10^{-8}	0.0	3.1	0.0019	6.3	6 3	1.1×10^{-5}
U(IV)	2.6×10^{-8}	0.0	0.0021	0.0021	6.3	6.3	1.1×10^{-5}
U(VI)	2.6×10^{-8}	0.0	0.0021	0.0023	0.12	0.51	1.1×10^{-5}
Np(IV)	2.6×10^{-8}	0.0	12.0	0.0027	6.3	6.3	1.1×10^{-5}
Np(V)	2.6×10^{-8}	0.0	12.0	0.0027	9.1×10^{-4}	7.4×10^{-3}	1.1×10^{-5}
Pu(III)	2.6×10^{-8}	0.0	0.3	6.8×10^{-5}	0.19	1.37[d]	1.1×10^{-5}
Pu(IV)	2.6×10^{-8}	1.0×10^{-9}	0.3	6.8×10^{-5}	6.3	6.3	1.1×10^{-5}
Am(III)	2.6×10^{-8}	0.0	3.6	NA	0.19	1.37[d]	1.1×10^{-5}

[a]In units of moles colloidal actinide per liter
[b]In units of moles colloidal actinide per mole dissolved actinide
[c]In units of moles total mobile actinide per liter
[d]A cumulative distribution from 0.065 to 1.60 with a mean value of 1.1 was used
NOTE: The colloidal source term is added to the dissolved source term to arrive at a total source term. Mineral fragments were provided with distributions, but the maximum was used as described in SOTERM.7.1.3. Humic proportionality constants for III, IV, and V were provided with distributions, but only the Castile Am(III) and Pu(III) were sampled.

4.2.1 Mineral fragment colloids

The mineral fragment colloid model considers the maximum concentration of actinides that may be mobilized by this type of colloid. The concentration of mineral fragment colloids is limited by the high ionic strength expected in the waters that may contact the waste (Section 2.2). The concentration of actinides adsorbed to these colloids is further limited by the specific surface area and sorption site density of the colloids.

For the CCA, experiments were performed to measure the stability of mineral fragment colloids in WIPP brines. The colloids tested included bentonite, kaolinite, montmorillonite, vermiculite, illite, anhydrite, calcium carbonate, magnesite, hematite, limonite, goethite, magnetite, quartz, siderite, brucite, strontianite, diatomaceous earth, pyrite, and cellulosic materials (DOE 1996, SOTERM.6.3.1). The brines included simulants of Salado groundwater, “Culebra brine,” and a NaCl-$CaCl_2$ solution. These brines were diluted sequentially to produce a set of solutions covering a broad range of salinity.

Stable mineral fragment colloid concentrations observed in solutions were converted to actinide concentrations by considering the surface area and sorption site density of the colloids. Assuming spherical particles, the associated (adsorbed) actinide concentrations, CONCMIN, were conservatively determined using the following relationship:

$$\text{CONCMIN} = \frac{\pi D^2 N_s N_p}{N_A} f_a f_c \qquad \text{(Eq. 3)}$$

where D is the particle diameter (nm), N_s is the adsorption site density (sites nm^{-2}), N_p is the number of particles per liter of solution determined in the laboratory experiments, N_A is the Avogadro constant, and f_a and f_c are factors used to conservatively account for additional mineral fragment colloids in the Culebra that might sorb actinides and for uncertainty, respectively. The final values determined for CONCMIN shown in

Table 4-2 assume

- 1 site nm^{-2} for N_s for each actinide,
- a particle concentration N_p equivalent to the observed geometric mean value for hematite, goethite, and bentonite, measured after 12.8 to 12.9 days in factor-of-10 diluted brine,
- a value of 2 for f_a to account for natural colloids potentially existing in the Culebra, and
- a value of 10 for f_c to account for uncertainty, mainly due to uncertainty in N_s (DOE 1996, SOTERM.6.3.1).

This calculation, its assumptions, and new data regarding the stability of mineral fragment colloids under WIPP conditions are examined in Section 5.1.4.

4.2.2 Intrinsic colloids

The intrinsic colloid model is based on intrinsic colloid solubility. Because the solubility of intrinsic colloids is generally low and depends on the oxidation state of the actinide, intrinsic colloids are assumed in the WIPP PA to be present at concentrations equal to their solubility. Accordingly, a single parameter is used in the model to represent the intrinsic colloid contribution to total mobile actinide concentrations: CONCINT, the molar concentration of the actinide associated with intrinsic colloids at its solubility limit at the specified oxidation state. This parameter is simply added to the other forms of mobile actinides to calculate total mobile actinide concentrations as shown in Eq. 1 and 2.

During the development of the WIPP colloid model, review of the literature and experimental studies conducted at Lawrence Livermore National Laboratory (LLNL) indicated that Pu(IV) was the only actinide and oxidation state in the WIPP waste inventory that could potentially form a significant concentration of intrinsic colloids under the alkaline conditions expected in the repository (DOE 1996, Section SOTERM.6.3.2). The experimental data produced a highly correlated linear inverse relationship between the log of the intrinsic colloid concentration and pcH (negative log of the concentration of hydrogen ion) over a range of pcH from 3 to 8.5 (DOE 1996, Figure SOTERM-8). These data are shown in Figure 4-1. Regression of this relationship indicates that Pu(IV) intrinsic colloid solubility is less than 3×10^{-10} M at the expected repository pcH of 9.3 (and much lower for the measurements in 5 M NaCl). Because the minimum analytical detection limit was 1×10^{-9} M, and this value is conservative relative to the regressed value, this limit was chosen as the Pu(IV) CONCINT value for the WIPP PA (

Table 4-2).

The value of CONCINT was set to zero in the CCA for all other actinides and oxidation states because of the absence of conclusive evidence of intrinsic colloids. In the CRA-2009, the CONCINT for Pu(III) was set to 1×10^{-9} M, removing the effects of oxidation state for Pu. Recent experimental studies at LANL provided new data on intrinsic colloid solubility under WIPP conditions (Reed et al. 2013a). These data, discussed in Section 5.2, led to recommended changes to the CONCINT values for all actinides for the CRA-2014 PA (Roselle 2013b).

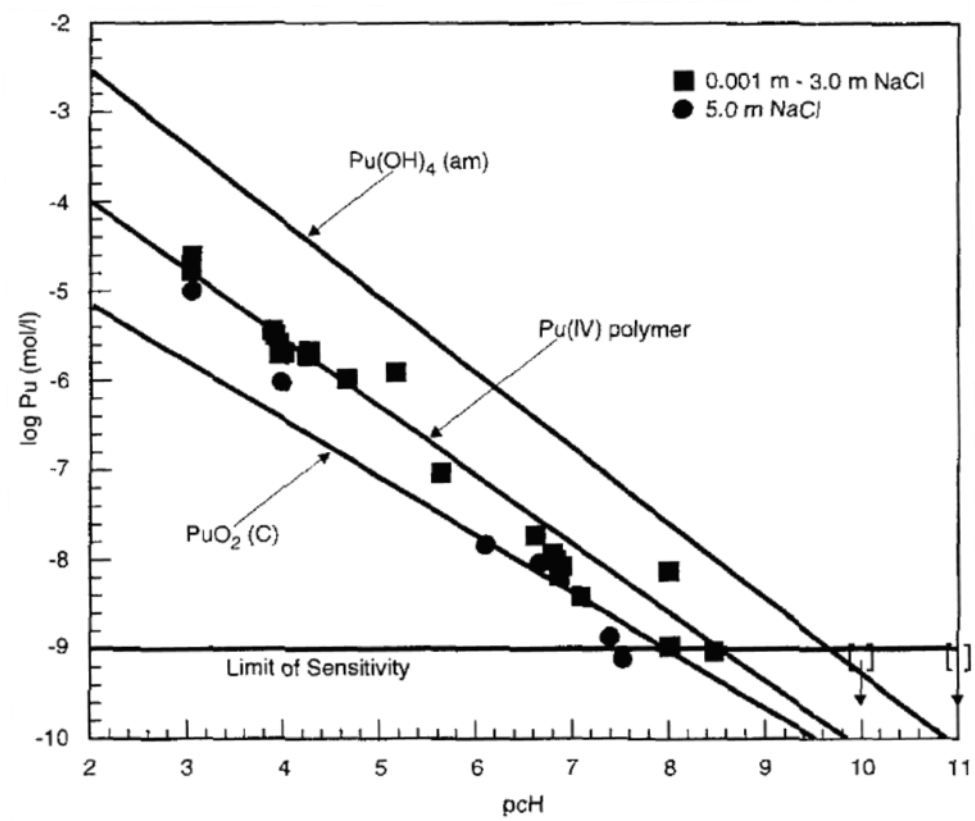

Figure 4-1. Solubility of Pu(IV)-polymer in NaCl media as a function of pcH (DOE 1996, Figure SOTERM-8).

4.2.3 Humic substance colloids

Two approaches were used to develop the model and parameters for the humic substance colloids in the CCA. For actinides at the IV oxidation state (i.e., Th(IV), U(IV), Np(IV), and Pu(IV)), a single value of 6.3 was calculated for the PHUMSIM and PHUMCIM proportionality constants (

Table 4-2). This calculation was based on the colloidal partitioning of Th(IV) in seawater reported in Baskaran et al. (1992) and assumes that the humic substance concentration in seawater is 2.0 mg L^{-1} (DOE 1996, SOTERM.6.3.3.1). For all other actinide oxidation states, a model was developed based on binary complexation data involving isolated humic substances. This latter approach produced an analytical model that includes actinide-humic complexation reactions and the competition for complexation sites by dissolved calcium (Ca^{2+}) and magnesium (Mg^{2+}).

The complexation of a dissolved actinide species (An^{m+}) with an available humic substance complexation site (HS^-) is described by the chemical reaction

$$\mathrm{An}^{m+} + m\mathrm{HS}^- \Leftrightarrow \mathrm{AnHS}_m \qquad \text{(Eq. 4)}$$

where AnHS_m is the actinide-humic substance complex. The stability constant ($\beta_{m:\mathrm{An}}$) for this chemical reaction is represented by

$$\beta_{m:\mathrm{An}} = \frac{[\mathrm{AnHS}_m]}{[\mathrm{An}^{m+}][\mathrm{HS}^-]^m} \qquad \text{(Eq. 5)}$$

where brackets denote equilibrium concentration of the species. For the CCA, humic complexation stability constants were determined for each actinide having oxidation states of III, V, and VI. Constants for the III and VI oxidation states were derived from laboratory experiments conducted at Florida State University as described below. For the V oxidation state, a stability constant of $10^{3.67}$ reported for Np(V) and Gorleben humic acid in a pH 9 solution was used (Kim and Sekine 1991).

Ca^{2+} and Mg^{2+} are abundant in the WIPP brines. The high concentrations of these cations and their affinity for humic complexation sites act to reduce the humic-bound concentrations of actinides. The WIPP colloid model for actinides at the III, V, and VI oxidation states accounts for this effect by including terms for humic-bound calcium and magnesium in the calculation of $[\mathrm{HS}^-]$. The model also assumes that (1) the concentration of An^{m+} is equal to the total dissolved non-colloidal concentration of An, (2) the combined total dissolved concentrations of Ca and Mg is equal to the combined concentrations of Ca^{2+} and Mg^{2+}, and (3) only 1:1 binding of An^{m+} and HS^- occurs (i.e., m is effectively assumed to be 1). These assumptions result in the following equation in the CCA for the concentration of HS^- (DOE 1996, Equation 6-20):

$$[\mathrm{HS}^-] = \frac{[\mathrm{HS}_{\mathrm{tot}}]}{\beta_{1:\mathrm{An}}[\mathrm{An}] + \beta_{1:\mathrm{CaMg}}[\mathrm{Ca}+\mathrm{Mg}] + 1} \qquad \text{(Eq. 6)}$$

$\beta_{1:\mathrm{CaMg}}$ is the combined stability constant for the humic complexation of Ca^{2+} and Mg^{2+}, $[\mathrm{Ca}+\mathrm{Mg}]$ is the sum of the dissolved Ca and Mg concentrations, $[\mathrm{HS}_{\mathrm{tot}}]$ is the total concentration of humic complexation sites, and $[\mathrm{An}]$ is the total dissolved non-colloidal concentration of actinide. In the CCA the log value for $\beta_{1:\mathrm{CaMg}}$ was set to 2.0 based on literature values from experiments investigating complexation of Ca^{2+} and $\mathrm{Mg}^{2+}$with humic and fulvic acids under acidic conditions in low-ionic-strength solutions (DOE 1996, SOTERM.6.3.3.1). The values for $[\mathrm{Ca}+\mathrm{Mg}]$ were taken from representative Salado and Castile brine compositions, 0.542 M and 0.0576 M, respectively (Papenguth 1996, Tables 1a and 1b); it is this term that explains the model dependence on the brine type.

The values used for $\beta_{1:\mathrm{An}}$ and $[\mathrm{HS}_{\mathrm{tot}}]$ in Eq. 6 were determined from experiments using Lake Bradford humic acid (HAal-LBr), Gorleben humic acid (HAal-Gor), and Suwannee River fulvic acid (FA-Suw). These experiments involved Am(III) and U(VI) in NaCl solutions of 3 and 6 molal. The pH values of these experiments were fixed in the acidic range at either 4.8 or 6 to maximize actinide complexation. Data from the 6 molal NaCl solutions at pH 6 were used in the derivation of the PHUMSIM and PHUMCIM proportionality constants. The site binding capacities of these humic substances were

determined to be 4.65, 5.38, and 5.56 meq g^{-1}, respectively. The concentration of humic substances in the Salado and Castile brines was set at the upper value (2.0 mg L^{-1}) of the solubility range observed in systems containing Ca^{2+} and Mg^{2+} at concentrations of at least 10 mM (DOE 1996, SOTERM.6.3.3.1). Multiplying this value by the site binding capacities gives the following values for $[HS_{tot}]$: 9.3×10^{-6} M (HAal-LBr), 1.1×10^{-5} M (HAal-Gor), and 1.1×10^{-5} M (FA-Suw).

Table 4-3 shows the values of $\beta_{1:An}$ and $[An]$ used in the derivation of the PHUMSIM and PHUMCIM values. The concentration of $[AnHS]$ in Table 4-3 is calculated by solving Eq. 5 for $[HS^-]$, substituting the result into Eq. 6, and solving for $[AnHS]$. This gives the following expression for $[AnHS]$:

$$[AnHS] = \frac{\beta_{1:An}[An][HS_{tot}]}{\beta_{1:An}[An] + \beta_{1:CaMg}[Ca + Mg] + 1} \qquad \text{(Eq. 7)}$$

This expression, which conservatively assumes that actinide species are monovalent and that there is no competition between actinides for binding sites, is used to calculate the $[AnHS]$ values shown in Table 4-3. The values in this table for $[An]$ are those assumed in the CCA for the brines in the Salado and Castile in the presence of MgO backfill (Papenguth 1996, Tables 1a and 1b).

The PHUMSIM and PHUMCIM values in

Table 4-2 for actinides at the III, V, and VI oxidation states were obtained by selecting the highest (most conservative) values of $[AnHS]/[An]$ in Table 4-3. Only the III oxidation state in the Castile brine was defined as a distribution. Based on the three values in Table 4-3 (0.065, 1.6, and 1.6), this distribution was defined with a minimum of 0.065, a mean of 1.1, a median of 1.37, and a maximum of 1.6 (Tierney 1996). It is a piecewise uniform distribution such that a random value between 0.065 and 1.37 is as equally likely as a random value between 1.37 and 1.6.

To ensure that calculations of humic-bound actinide concentrations (Eq. 7) are not excessive, a maximum concentration parameter called CAPHUM was defined in the CCA to set the upper limit. The value of this parameter was set at 1.1×10^{-5} M, which is the maximum $[HS_{tot}]$ value used in the calculations in Table 4-3. This is a conservative value because it assumes that actinide species are monovalent and that there is no competition between actinides for binding sites. In the event that a calculation using PHUMSIM or PHUMCIM and the dissolved actinide concentration exceeds CAPHUM, the WIPP PA sets the humic-bound actinide concentration at CAPHUM.

The values of the PHUMSIM, PHUMCIM, and CAPHUM used in the WIPP PA are examined in Section 5.3.4 in light of their inherent assumptions and with respect to new data.

Table 4-3. Calculated values of humic-bound actinide concentrations $[AnHS]$ and proportionality constants (i.e., PHUMSIM and PHUMCIM) for U(VI), Np(V), and Am(III). Inputs from Papenguth (1996, Tables 1a, 1b, and 3)

Formation	Actinide	$[An]$ (M)	Humic Substance	$[HS_{tot}]$ (M)	log $\beta_{1:An}$	$[AnHS]$ (M)	$[AnHS]/[An]$
Salado	U(VI)	1.00E-05	HAal-LBr	9.3E-06	5.91	1.2E-06	0.12
			HAal-Gor	1.1E-05	5.35	4.2E-07	0.042
			FA-Suw	1.1E-05	4.60	8.0E-08	0.0080
	Np(V)	2.64 E-06	HAal-Gor	1.1E-05	3.67	2.4E-09	9.1E-04
	Am(III)	4.39 E-06	HAal-LBr	9.3E-06	6.09	8.3E-07	0.19
			HAal-Gor	1.1E-05	6.02	8.3E-07	0.19
			FA-Suw	1.1E-05	4.60	3.5E-08	0.0080
Castile	U(VI)	1.00E-05	HAal-LBr	9.3E-06	5.91	5.1E-06	0.51
			HAal-Gor	1.1E-05	5.35	2.7E-06	0.27
			FA-Suw	1.1E-05	4.60	6.2E-07	0.062
	Np(V)	2.53 E-06	HAal-Gor	1.1E-05	3.67	1.9E-08	7.4E-03
	Am(III)	4.12 E-07	HAal-LBr	9.3E-06	6.09	6.5E-07	1.6
			HAal-Gor	1.1E-05	6.02	6.5E-07	1.6
			FA-Suw	1.1E-05	4.60	2.7E-08	0.065

4.2.4 Microbial colloids

Like the humic substance colloid model, the microbe colloid model for the WIPP PA uses a proportionality constant (PROPMIC) and a maximum associated actinide concentration (CAPMIC). These constants are used in the WIPP PA in the same way as the humic colloid constants (Section 4.2.3). PROPMIC differs from the humic proportionality constant in that it depends on the element and not the oxidation state. CAPMIC differs from its humic counterpart in that its value reflects the observed bioaccumulation and toxicity of the element.

For the CCA, filtration experiments were conducted at Brookhaven National Laboratory and LANL to measure mobile indigenous microbial concentrations (DOE 1996, SOTERM.6.3.4.1). These experiments combined ^{232}Th, ^{238}U, ^{237}Np, ^{239}Pu, or ^{243}Am at various concentrations (with and without organic complexants such as EDTA) with two different microbe cultures that tolerate high salinity. A culture called WIPP-1A is fast growing and was used for the majority of the experiments. This culture was isolated from saline surficial sediments at the WIPP site and prepared in a medium containing 200 g L^{-1} NaCl (Gillow et al. 1998). The other culture, called BAB, required several weeks to reach steady state.

The concentrations of mobile colloids were determined by measuring the mobile cells that remained suspended after 11 to 15 days in the WIPP-1A mixed culture and after as many as 21 days in the BAB mixed culture. A filtration sequence of 0.03 µm, 0.4 µm, and 10 µm was used to determine the dissolved actinide and microbial actinide concentrations. PROPMIC was set by the ratio of microbial actinide to dissolved actinide. Results from the BAB experiments were not used in the PROPMIC calculations because of low uptake (especially of plutonium) and the limited number of experiments conducted using the BAB mixed culture.

CAPMIC values were determined from the filtration experiments by measuring the actinide concentrations at which no microbial growth was observed (DOE 1996, SOTERM.6.3.4.1). In cases where growth was observed to decrease but not stop, CAPMIC was determined by extrapolation and an order-of-magnitude addition for uncertainty. In the case of Am(III), in which no decrease in microbial concentrations was observed with increases in actinide concentrations, no limit was set in the CCA. A CAPMIC value of 1 M, however, was observed in the CRA-2009 for Am(III) (DOE 2009, Table SOTERM-23). Uncertainty distributions were not established for either PROPMIC or CAPMIC in the PA.

In the CRA-2014 PA, the same general parameters and equations were used to calculate microbially-bound actinide concentrations. However, as discussed in Section 5.4, the values of these parameters were changed based on the data and analyses presented in Reed et al. (2013a).

4.3 WIPP Colloid Model Results

The relative abundances of the colloidal and dissolved actinides for the CCA in the direct brine release (DBR) scenario are shown in Figure 4-2 for Castile and Salado dominated brines. This figure shows that colloidal contributions were particularly important for Am, Pu, and Th in the CCA via a variety of colloidal types. Microbial colloids were the dominant contributors to total mobile concentrations for Am in both brines and for Th in the Salado brine. Humic colloids were dominant or substantial contributors for Pu and Th in both brines, for Am in Castile brine, and for U for Salado brine. Mineral fragment colloids had negligible contributions for all actinides except for Th in the Castile brine. Figure 4-2 further indicates that for all actinides, there was no substantial contribution by intrinsic colloids to total mobile concentrations in the CCA.

From a regulatory perspective, based on the realized EPA units per cubic meter (Figure 4-2), Am and Pu were the most important constituents for the DBR scenario in the CCA. Because only organic colloids contributed substantially to total mobile concentrations of Am and Pu, the organic colloids were the only colloids that had a significant effect on the WIPP PA results.

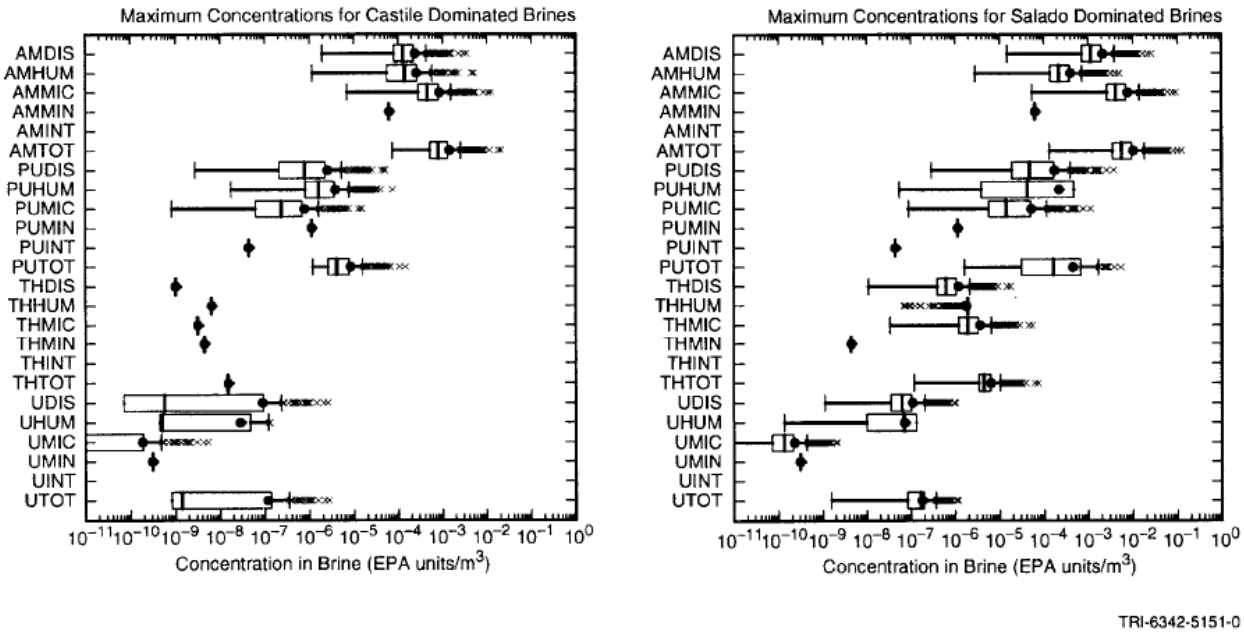

Figure 4-2. CCA results for direct brine release to the Culebra in terms of source constituents (Helton et al. 1998, Figure 11.1.1).

5 WIPP COLLOID PARAMETER ANALYSES

5.1 Mineral Fragment Colloids

5.1.1 EPA Comments

In a letter to the DOE on February 22, 2010, the EPA made the following comment with respect to intrinsic and mineral fragment colloids (Kelly 2010, Comment 4-C-36):

> DOE should address whether significant thorium intrinsic colloids and pseudocolloids could form in the WIPP repository. Unless the formation of such colloids can be ruled out by the available data, DOE should address the possible effects of such colloid formation on repository performance.

This comment was spurred by the results of Altmaier et al. (2004) which found high concentrations of Th(IV) intrinsic colloids and pseudocolloids of korshunovskite ($Mg_2Cl(OH)_3{\cdot}4H_2O$, also known as "phase 3"). With respect to thorium pseudocolloids, Xiong et al. (2010a) explained that phase 3 is not relevant to the WIPP. Experimental results show that in WIPP brines phase 5 ($Mg_3(OH)_5Cl{\cdot}4H_2O$) forms, which is consistent with thermodynamic calculations. The EPA in its Chemistry Technical Support Document (EPA 2010) expressed additional interest in Mg-Cl-OH pseudocolloids.

5.1.2 Current PA Representation

In the development of the CCA model a number of possible phases including clays, sulfates, carbonates, and iron oxides mineral fragment colloids, were considered. Experiments were conducted to characterize concentrations of actinides associated with these phases in simulated 10-fold-diluted WIPP brines (Section 4.2.1). Averages of the concentrations of hematite, goethite, and bentonite colloids measured in those experiments led to the ultimate CONCMIN parameter value constraining the concentrations of each actinide bound to mineral fragment colloids to $2.6{\times}10^{-8}$ M. As explained in Section 4.2, a number of assumptions, many of them conservative, were used to establish this value for CONCMIN. These assumptions are evaluated in Section 5.1.4.

5.1.3 Literature Review

In 2004, a publication on the solubility of Th(IV) in brines by Altmaier et al. (2004) indicated high concentrations of colloidal Th(IV) in carbonate-free NaCl or $MgCl_2$ solutions equilibrated with brucite ($Mg(OH)_2$(cr)) or magnesium hydroxychloride ($Mg_2(OH)_3Cl{\cdot}4H_2O$(cr)) (i.e., "phase 3"). In one set of experiments, Th(IV) was introduced into solutions undersaturated with Th(IV) via addition of excess ThO_2(cr) or $ThO_n(OH)_{4-2n}{\cdot}xH_2O$(am). Samples in the $Th(OH)_4$(am) solubility experiments were equilibrated for 20 to 100 days before they were ultracentrifuged to separate intrinsic Th(IV) colloids from the remaining dissolved Th(IV). In a separate set of experiments, solubility measurements were conducted from the direction of oversaturation via NaOH titration. Samples from this latter set of experiments were equilibrated for one day prior to ultracentrifugation.

Two types of colloids were identified in the Altmaier et al. (2004) study, intrinsic Th(IV) colloids (called eigencolloids in the article) and magnesium hydroxychloride mineral fragment colloids. The intrinsic colloids formed in each of the experiments and could be separated by ultracentrifugation due to density differences between the colloids and the solutions. The pseudocolloids occurred only in experiments involving 2.5 M and 4.5 M $MgCl_2$ solutions. Their presence was largely responsible for the high range of Th(IV) concentrations ($10^{-7.9}$ to $10^{-6.4}$ M) observed in the ultracentrifuged samples from the undersaturation $Th(OH)_4$(am) solubility experiments in the 2.5 M and 4.5 M $MgCl_2$ solutions. After 10 kD (2 nm) ultrafiltration, the dissolved Th(IV) concentration in the 4.5 M $MgCl_2$ solution dropped from $10^{-6.4}$ M to $10^{-8.1}$ M. Pseudocolloids were also studied in oversaturation experiments in which the colloids

were formed in the presence of Th(IV). The study concludes that the high Th(IV) concentrations observed for these mineral fragment colloids are not expected in real systems because real systems with 2.5 M and 4.5 M $MgCl_2$ would have a large ratio of solid (immobile) magnesium hydroxychloride phase relative to the aqueous phase, which would reduce concentrations of Th(IV) associated with colloids.

Mg-Cl-OH colloids were not investigated as potential mineral fragment colloids in the CCA (DOE 1996). After the Altmaier et al. (2004) study was published, SNL began laboratory experiments to test the stability of such colloids in WIPP brines in the presence of periclase (MgO) and brucite ($Mg(OH)_2$). In GWB, hydration of either periclase or brucite was found to produce phase 5 in the presence of an atmospheric concentration of CO_2 (~4×10^{-4} atm) but no Mg-Cl-OH phase at a CO_2 partial pressure of 5×10^{-2} atm (Xiong and Lord 2008). No Mg-Cl-OH phases precipitated in any of the hydration experiments involving ERDA-6 regardless of CO_2 partial pressure (Xiong and Lord 2008). Because the rates of carbonation of brucite are much higher than the rates of possible CO_2 generation by microbial activity, the lower atmospheric CO_2 partial pressure is expected to be more relevant to WIPP conditions. Thus, for Mg-Na-Cl-dominated brines such as GWB, formation of phase 5 is expected under repository conditions. Subsequent SNL laboratory work indicates that phase 5, not phase 3, is the stable Mg-Cl-OH phase in Mg-Na-Cl-dominated brines in the presence of periclase or brucite (Xiong et al. 2010b).

Solubility experiments were conducted at LANL for Nd(III), Th(IV), and U(VI) using GWB and ERDA-6 at pcH values between 7 and 12 and varying concentrations of carbonate and organic complexants (Reed et al. 2013a; Borkowski et al. 2012). Based on negligible differences in concentrations of actinides observed in unfiltered samples and samples that filtered out colloids of size 10 nm and greater, Reed et al. (2013a) concluded that mineral fragment colloids appear to be an insignificant component of mobile actinide concentrations in WIPP brines.

Though Mg-Cl-OH colloids may not be significant in undiluted WIPP brines, significant concentrations of Pu were associated with mineral fragment colloids in iron corrosion experiments in WIPP brines (Reed et al. 2013a, Section 4.2.3; LANL 2010, Section 4.3). In these experiments, which lasted nearly six years, iron coupons were placed in WIPP brine containing ~5×10^{-5} M Pu(VI). As the iron oxidized, the aqueous Pu(VI) reduced to Pu(IV) mineral phases (LANL 2010, Figure 4-13) and predominantly to Pu(III) aqueous species (Reed et al. 2013a, Table 4-3). Samples of the solution were filtered sequentially using 0.45 μm, 0.22 μm, 20 nm, 10 nm, 5 nm, and 2.5 nm filters. Intrinsic colloids were defined to be those in the range of 2.5 to 10 nm, and mineral fragment colloids were defined to be those in the range of 10 nm to 0.45 μm. Based on this distinction, Pu concentrations associated with mineral fragment colloids in the samples identified to be most repository-relevant (i.e., the three ERDA-6 samples with pcH values in the range of 9.1 to 9.6) ranged from 8.6×10^{-9} to 2.3×10^{-8} M (Reed et al. 2013a, Table 4-4).

Prediction of mineral fragment colloid stability has been advanced by Abdel-Fattah et al. (2013). The Hamaker constant is needed to calculate van der Waals interactions between colloids, including natural groundwater colloids, and between colloids and surfaces of the porous medium. Abdel-Fattah et al. (2013) used this constant to develop response surfaces as a function of pH and ionic strength to show where energy barriers to aggregation are high between colloids of the same type, between colloids of different type, and between colloids and stationary surfaces. The results indicate that at high ionic strength and high pH the energy barrier for the aggregation of smectite colloids, Pu intrinsic colloids, and smectite colloids with Pu intrinsic colloids is very low. Bentonite, an impure clay consisting mostly of montmorillonite (a smectite), was found to provide stable colloids after 12.8 to 12.9 days in factor-of-10 diluted WIPP brines (Section 4.2.1). A potential source of bentonite in the direct brine release scenario is the common use of bentonite in drilling muds. Energy barriers involving other types of colloids were not analyzed in the Abdel-Fattah et al. (2013) study.

5.1.4 Analysis

5.1.4.1 Mg-Cl-OH phases relevant to WIPP

The Mg-Cl-OH colloids observed in Altmaier et al. (2004) were phase 3, $Mg_2Cl(OH)_3{\cdot}4H_2O$. This phase precipitated in carbonate-free NaOH solutions containing excess $Mg(OH)_2$ (cr) and 2.5 or 4.5 M $MgCl_2$. Precipitation of phase 3 in these solutions is consistent with thermodynamic model calculations for brines having high Mg concentrations and high pH. Xiong et al. (2010b) show that for the Q-brine of the Asse repository, phase 3 is predicted to be the stable phase. However, in the presence of additional alkalinity from, for example, cemented waste forms and additional MgO buffer material, phase 5 could become the stable Mg-Cl-OH phase (Xiong et al. 2010b).

WIPP conditions are different from conditions expected in the Asse repository where $Mg(OH)_2$, not MgO, is the emplaced buffer material. In brines like GWB in the presence of a low partial pressure of CO_2 (e.g., atmospheric), $Mg_3(OH)_5Cl{\cdot}4H_2O$ (phase 5) is thermodynamically stable, and laboratory experiments confirm that it precipitates (Xiong and Lord 2008). Thus, phase 5 is the mineral phase of Mg-Cl-OH that would be expected to be thermodynamically stable in the WIPP repository. Whether colloids of phase 5 are electrostatically stable depends on the energy barrier to phase 5 particle aggregation under these conditions.

In the presence of ERDA-6, however, no Mg-Cl-OH mineral phase is predicted to be thermodynamically stable, and no Mg-Cl-OH mineral phase is observed to precipitate in laboratory experiments (Xiong and Lord 2008). Thus, no Mg-Cl-OH colloids are expected to be thermodynamically stable in scenarios involving ERDA-6. Whether such colloids may be metastable at low concentrations, however, remains a possibility.

5.1.4.2 Concentrations of Mg-Cl-OH colloids relevant to WIPP

The concentrations of Th(IV) associated with the phase 3 colloids in the undersaturation experiments of Altmaier et al. (2004) were as high as $10^{-6.4}$ M. These colloids only occurred in samples containing 2.5 and 4.5 M $MgCl_2$ solution, and their concentrations were especially high in the 4.5 M $MgCl_2$ solution. Subsequent one-day oversaturation experiments using 4.5 M $MgCl_2$ confirmed the formation of phase 3 colloids, but because the formation of colloids is not expected to be from oversaturation in a repository setting (i.e., formation due to addition of NaOH in the presence of dissolved Th(IV) and possible incorporation of Th(IV) within the colloid itself), the concentrations of Th(IV) in pseudocolloids measured in the oversaturation experiments are not expected to be relevant to the prediction of the pseudocolloid component of Th(IV) releases from a repository.

The measurements of Th(IV) associated with phase 3 mineral fragment colloids in the 4.5 M $MgCl_2$ solution in the undersaturation experiments were taken after 100 days of equilibration with excess $Th(OH)_4$(am) and brucite (Altmaier et al. 2004, Table 3). It is possible that these colloids were slowly aggregating and that they were decreasing with time. Energy barriers to aggregation are low at high ionic strength, but aggregation rates may be diffusion limited due to the low concentrations of the colloids(Abdel-Fattah et al. 2013).

In WIPP brines, the only Mg-Cl-OH phase that is thermodynamically stable is phase 5 and it is only stable in GWB in the presence of MgO or $Mg(OH)_2$ (Section 5.1.4.1). However, Mg-Cl-OH colloids have not been observed in any experiments involving WIPP brines. These experiments include the hydration experiments of Xiong and Lord (2008) and Xiong et al. (2010b) and LANL solubility experiments of Nd(III), Th(IV), and U(VI) (Borkowski et al. 2012; Reed et al. 2013a). Based on the actinide concentrations observed in solubility experiments after ultracentrifugation and ultrafiltration, actinide association with pseudocolloids under WIPP chemical conditions appears to be insignificant (Reed et al. 2013a).

5.1.4.3 Concentrations of mineral fragment colloids observed in nature

Though Mg-Cl-OH mineral fragment colloids are not expected to occur in significant concentrations in WIPP PA release scenarios, other types of mineral fragment colloids have shown potential for significant stability in WIPP brines. Laboratory studies conducted for the CCA indicate that among a broad list of potential mineral colloids, colloids of hematite, goethite, and bentonite showed some stability in 10-fold diluted WIPP brines (Section 4.2.1). In addition to potential natural groundwater colloids, colloids in the WIPP repository may be generated by microbial activity and corrosion of waste forms and waste materials. Microbial degradation of organic materials can generate humic substance colloids, and corrosion of solids such as steel can generate iron oxide colloids. Organic colloids are addressed in Sections 5.3 and 5.4, and iron oxide colloids generated from active corrosion is addressed in Section 5.1.4.4.

Concentrations of mineral fragment colloids in natural groundwaters and simple salt solutions are observed to vary by orders of magnitude. Figure 5-1 presents a plot prepared by Serco that shows a compilation of colloid concentrations measured in natural systems and simple salt solutions as function of ionic strength (Alexander et al. 2011, Figure 5.1). Hatched red, blue, and gray regions indicate ranges observed at Grimsel, Ruprechtov, and Äspö, yellow triangles represent measurements largely from granitic groundwaters, and circles and diamonds represent colloids in simple salt solutions.

Consistent with DLVO theory (Section 2.2), measurements of high colloid concentrations in the Serco plot are noticeably absent at high ionic strength (>0.2 M). Much of the scatter in the plot at lower ionic strength is attributed to different solution compositions, pH values, and sampling procedures. Some of the scatter at lower ionic strength may also be the result of the association of mineral fragment colloids with other types of colloids that can act to stabilize mineral fragment colloids in solution (Borgnino 2013; Abdel-Fattah et al. 2013).

The range of concentrations of mineral fragment colloids simulated in the WIPP PA is approximately 40 to 400 μg L^{-1}. Because the ionic strength of WIPP brine is in the vicinity of 6,000 mmol L^{-1}, this range of colloid concentrations would plot to the right of the data shown in Figure 5-1. This range was calculated assuming the following:

- Each of the five actinide elements (Th, U, Np, Pu, and Am) sorb at a site density (N_s) of 10 nm^{-2}.
- The colloids are spherical and have a representative diameter (D) of between 10 and 100 nm.
- The colloid solid density is 3 g mL^{-1}.

The first assumption is consistent with assumptions used in the original calculation of CONCMIN; specifically, the site density for each actinide is equivalent to the originally assumed 1 nm^{-2} site density multiplied by the uncertainty factor of 10 included in the CONCMIN calculation. Because the mineral fragment colloid model assumes that all surface sites are occupied by the five actinide elements (except when the system is limited by the actinide inventory), the total concentration of actinides associated with mineral fragment colloids in the WIPP PA model is five times CONCMIN. The second and third assumptions are used to estimate a colloid concentration (C_c) in units of mass colloids per volume of water (e.g., μg L^{-1}). The calculation is made using the following equation:

$$C_c = \frac{5\ \mathrm{CONCMIN}\ N_A\ \rho_c D}{6\ N_s} \qquad \text{(Eq. 8)}$$

Where 5 CONCMIN is the total concentration of the five actinides associated with mineral fragment colloids (1.3×10^{-7} M), ρ_c is the colloid solid density (3 g mL^{-1}), and $D/6$ is the ratio of the colloid particle volume to its surface area. Varying the colloid diameter between 10 and 100 nm gives the calculated 40 to 400 μg L^{-1} concentrations effectively used in the WIPP PA.

This effective concentration range for mineral fragment colloids appears to be highly conservative for high-ionic-strength brines. The lower end of the range (40 μg L^{-1}) is ~2,000 times higher than any of the data in the Serco plot for ionic strength greater than 0.2 M and ~4,000 times higher than the 0.01 μg L^{-1} colloid concentration used for the Yucca Mountain PA (Buck and Sassani 2007). The only mineral fragment colloid measurements that approach this range for undiluted WIPP brines are those observed to be generated in iron corrosion experiments where soluble Pu(VI) is reduced to insoluble Pu(IV) (Section 5.1.4.4).

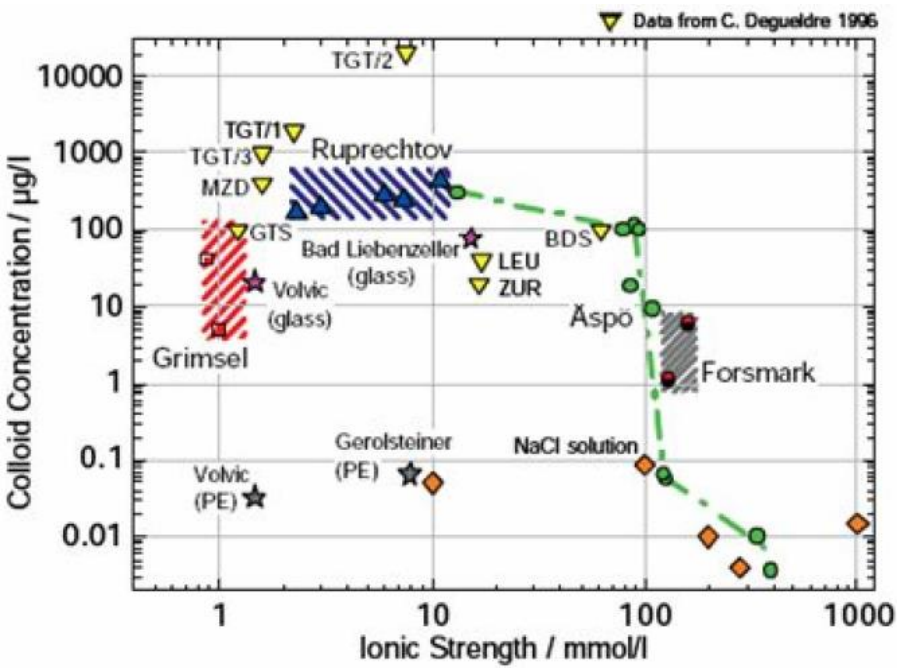

Figure 5-1.Colloid concentrations from natural systems and simple salt solutions as function of ionic strength as compiled by Serco (Alexander et al. 2011, Figure 5.1).

5.1.4.4 Effect of corrosion on mineral fragment colloid concentrations

The Pu concentrations observed in the 10 nm to 0.45 μm fraction of the long-term Pu-iron interaction experiments (8.6×10^{-9} to 2.3×10^{-8} M) are nearly as high as the 2.6×10^{-8} M value set for CONCMIN (Reed et al. 2013a, Section 4.2.3; Reed et al. 2013b). As shown in the previous section, the CONCMIN value is consistent with assuming a colloid concentration in the range of 40 to 400 μg L^{-1}, which is much higher than colloid concentrations typically observed in highly saline waters.

One explanation for the high concentrations of Pu in the 10 nm to 0.45 μm fraction may be continuous corrosion of iron in these experiments. Continuous corrosion could generate a continuous supply of colloids which could support a relatively high, steady-state concentration of mineral fragment colloids and therefore a high concentration of Pu associated with these colloids. Continuous corrosion would require a continuous supply of oxidants (e.g., via radiolysis). A steady high concentration of colloids could therefore be maintained by a balance between colloid generation rates and rates of colloid aggregation and flocculation.

A more likely explanation for the high concentration of Pu in the 10 nm to 0.45 μm size fraction is that much of it may have been in mineral form. Addition of the iron coupons in these experiments caused the aqueous Pu(VI) to reduce and to precipitate as Pu(IV) mineral phases (LANL 2010, Figures 4-12 and 4-13). This Pu(IV) mineral phase was closely associated with the formation of green rust on the iron coupons. Steel corrosion in WIPP brines have been found to produce a green Fe(±Mg)-chlori-hydroxide phase at low CO_2 concentrations (<1500 ppm) and a Fe-Mg-Ca hydroxicarbonate phase at higher CO_2

concentrations (Roselle 2013a). Thus, the mineral fragment colloids that were isolated in the Pu-iron interaction experiments may have included Pu(IV) mineral phases and/or Pu(IV) otherwise incorporated into colloid structures. In addition, intrinsic Pu(IV) colloids may attach to mineral fragment colloids and thereby be retained in the 10 nm to 0.45 µm size fraction. If it is true that the bulk of the Pu in the 10 nm to 0.45 µm size fraction is not sorbed but rather is in mineral form, then the observed Pu concentrations in this size fraction could have been associated with a very low concentration of mineral fragment colloids, as might be expected in a highly saline system at equilibrium or under conditions of very low corrosion rates.

The generation of Pu(IV) mineral phases in the Pu-iron interaction experiments are a result of oversaturation caused by the introduction of zero-valent iron and subsequent reduction of Pu(VI). This sequence of events could potentially occur in isolated microenvironments with high Pu loadings where considerable radiolytic oxidation could occur.

5.1.4.5 Assessment of conservatism in WIPP mineral fragment colloid model

The mineral fragment colloid model for the WIPP PA is based on two conservative model assumptions and three conservative assumptions used to calculate CONCMIN. The conservative model assumptions are

- Mineral fragment colloids will be fully loaded. The actinide concentration associated with these colloids will be a constant value (CONCMIN) and equals the concentration of surface sites on these colloids (Section 4.2.1). In reality, actinides will partition between the aqueous phase and colloid surface sites (generally in proportion to aqueous actinide concentrations, and will depend on aqueous composition) and will not occupy all of the surface sites. The amount of conservatism owing to this assumption can only be determined by detailed study.
- Mineral fragment colloids will be fully loaded with *each* actinide. Because there are 5 primary actinides in the WIPP colloid model (Th, U, Np, Pu, and Am), this assumption means that the total concentration of actinides sorbed to mineral fragment colloids is 5 times greater than the mineral fragment colloid surface site concentration, i.e., 5 times CONCMIN.

The value determined for CONCMIN (2.6×10^{-8} M) for each actinide is set equal to a mineral fragment colloid surface site concentration, which was determined based on measurements of mineral fragment colloid particles in dilute WIPP brine and conservative assumptions regarding the surface site concentration associated with these particles. The conservative assumptions used to calculate CONCMIN include the following:

- The particle concentration in WIPP brines is equivalent to the observed geometric mean value for hematite, goethite, and bentonite measured after 12.8 to 12.9 days in factor-of-10 diluted brine. This assumption is conservative because undiluted WIPP brines and longer equilibration times would have resulted in lower observed particle concentrations. In the experimental work, there was a notation that the colloidal components were flocculating rapidly in the brines (Papenguth and Behl, 1996). This is expected as discussed above regarding the expected instability of colloids in such brines; however without a long-term benchmark the short term experiments were used as the basis for the parameter value.
- A factor of 2 was added to the site concentration to account for natural colloids potentially existing in the Culebra. This adjustment is conservative because not all releases occur in the Culebra, and for those that do, there is little evidence that they would enhance the mineral fragment component of total mobile actinide concentrations.
- An additional factor of 10 was added to the site concentration to account for uncertainty (Section 4.2.1). This factor is a direct conservative assumption.

The five conservative assumptions listed above are independent and multiplicative and likely result in predicted actinide concentrations associated with mineral fragment colloids that are at least two orders of magnitude above expected values. Based on the trends in Figure 5-1, these predicted concentrations may actually be at least three orders of magnitude too high.

5.1.5 Conclusions

5.1.5.1 The value of CONCMIN should not be increased to account for potential Mg-Cl-OH colloids.

Mg-Cl-OH colloids have not been observed in hydration and solubility experiments involving WIPP brines and have not been observed in concentrations approaching CONCMIN (Section 5.1.4.2). Thus, there is no reason to increase the value of CONCMIN to account for potential Mg-Cl-OH colloids.

5.1.5.2 The value of CONCMIN for each actinide element could justifiably be reduced, but doing so would have little effect on WIPP releases.

The CONCMIN value of 2.6×10^{-8} M was determined based on conservative assumptions that were applied to concentration measurements of hematite, goethite, and bentonite colloids in 10-fold diluted WIPP brine. The analyses in Sections 5.1.4.3 and 5.1.4.5 indicate that a more realistic estimate of the mineral fragment contribution to mobile actinide concentrations is likely at least two orders of magnitude lower than the current value of CONCMIN but perhaps not assuredly so without additional supporting evidence. However, because the contributions of mineral fragment colloids to total actinide release calculations are minor (Section 4.3), reducing the conservatisms in the CONCMIN values would have an insignificant effect on calculated WIPP releases.

5.1.5.3 The predominant phases of Pu (sorbed and/or mineral) associated with colloids in Pu-iron interaction studies should be investigated.

Although the association of Pu with mineral fragment colloids in iron corrosion experiments in WIPP brines appear to support the current value of CONCMIN, the form of Pu associated with these colloids has not been fully investigated (Section 5.1.4.4). In the experiments, dissolved Pu(VI) is reduced by the introduction of the iron coupon and rapid precipitation of Pu(IV) ensues. It is conceivable therefore that much of the Pu observed in the 10 nm to 0.45 μm size fraction may exist as Pu(IV) mineral phases and intrinsic colloids attached to mineral fragment colloids. If this is true, then these colloids would be specific to Pu and more appropriately modeled as Pu intrinsic colloids.

5.2 Intrinsic Colloids

5.2.1 EPA Comments

As stated in Section 5.1.1, the EPA asked the DOE to address thorium intrinsic colloids and whether a significant amount of these colloids could form in the WIPP repository (Kelly 2010, Comment 4-C-36). In the response by the DOE, Xiong et al. (2010a) noted that intrinsic colloid data for Th(IV) in WIPP brines were not available and that the data provided by Altmaier et al. (2004) were for pure NaCl or $MgCl_2$ solutions. Xiong et al. (2010a) also noted that the higher non-ultracentrifuged Th(IV) concentrations from Altmaier et al. (2004), which included intrinsic colloids, were conservatively included in the WIPP Th(IV) solubility uncertainty analysis instead of the much lower concentrations measured after ultracentrifugation. Additional analysis is presented in Section 5.2.4.

In the Technical Support Document (TSD) for Section 194.24, the EPA evaluated the potential effects on performance assessment results by including Th(IV) data reported in Altmaier et al. (2004). The EPA used Table SOTERM-25 (DOE 2009, Appendix SOTERM-2009) that provided values of dissolved and

colloidal actinide concentrations based on the median parameter values for the CCA PA (DOE 1996) and the CRA-2004 PA baseline calculations (DOE 2004) summarizing those values in Table 8.1 (EPA 2010). The results of the EPA sensitivity study (which also included changes for dissolved actinide concentrations), were summarized in Table 8.2 (EPA 2010).

For the concentrations of dissolved Th(IV) and Th(IV) associated with intrinsic colloids, the EPA used the measurements of Altmaier et al. (2004), i.e., 8.49×10^{-10} M and 5.01×10^{-7} M, respectively. The results showed increased mobilized concentrations of Th(IV) in the Salado and Castile by factors of 1.85 and 1.52, respectively. Much of the increase from the intrinsic colloid component was offset by decreases in the dissolved, humic, and microbial components. The humic colloid Th(IV) concentration decreased from 1.60×10^{-7} M (Salado) and 1.98×10^{-7} M (Castile) to 5.35×10^{-9} M (both), while the microbial colloid Th(IV) concentration decreased from 7.87×10^{-8} M (Salado) and 9.75×10^{-8} M (Castile) to 2.63×10^{-9} M (both). The humic and microbial Th(IV) concentrations decreased because they are calculated as being proportional to the dissolved Th(IV) concentrations, as discussed in Section 4.2. The EPA concluded that the effects on PA results were relatively small because of the minor inventory of Th(IV) in the WIPP waste forms (as compared to Am and Pu). In its evaluation, the EPA indicated that further evaluation was needed to rule out intrinsic thorium colloids as relevant to the WIPP repository.

5.2.2 Current PA Representation

Until the CRA-2014 PA, Pu intrinsic colloids were the only intrinsic colloids explicitly included in the WIPP PA (Section 4.2.2). For the CRA-2014 PA, the following CONCINT values are used: 2×10^{-8} M for Th, Np, and Pu, 3×10^{-8} M for U, and 4×10^{-9} M for Am (Roselle 2013b). These values originate from recommendations in Reed et al. (2013a) and are based on recent measurements of intrinsic colloids in WIPP-relevant brines.

5.2.3 Literature Review

In 2004, the Altmaier et al. (2004) publication indicated high concentrations of Th(IV) intrinsic colloid in carbonate-free NaCl or $MgCl_2$ solutions equilibrated with brucite ($Mg(OH)_2$(cr)) or magnesium hydroxychloride ($Mg_2(OH)_3Cl{\cdot}4H_2O$(cr)) (i.e., "phase 3"). In one set of experiments, Th(IV) was introduced into solutions undersaturated with Th(IV) via addition of excess ThO_2(cr) or $ThO_n(OH)_{4-2n}{\cdot}xH_2O$(am). Samples in the $Th(OH)_4$(am) solubility experiments were equilibrated for 20 to 100 days before they were ultracentrifuged to separate intrinsic Th(IV) colloids from the remaining dissolved Th(IV). In a separate set of experiments, solubility measurements were conducted from the direction of oversaturation via NaOH titration. Samples from this latter set of experiments were equilibrated for one day prior to ultracentrifugation.

Intrinsic colloids formed in each of the Altmaier et al. (2004) experiments and could be separated by ultracentrifugation due to density differences between the colloids and the solutions. The noncolloidal fractions in the experiments that did not have magnesium hydroxychloride mineral fragment colloids (i.e., 0.5M NaCl, 5.0 M NaCl, and 0.25 M $MgCl_2$ solutions) were found to have concentrations in the range of approximately $10^{-9.1}$ M to $10^{-8.3}$ M (Altmaier et al. 2004, Table 2). This range is comparable to the solubility of $Th(OH)_4$(am) ($10^{-8.5}$ M) (Neck and Kim 2001) and also to the range of Th(IV) solubilities found in other studies (Altmaier et al. 2004, Figure 2). In these same solutions, intrinsic colloids were measured to have concentrations in the range of $10^{-7.3}$ M to $10^{-6.3}$ M (Altmaier et al. 2004, Table 2). In the corresponding one-day oversaturation experiments, a higher range of concentrations of intrinsic colloids was measured ($10^{-6.6}$ M to $10^{-5.6}$ M) (Altmaier et al. 2004, Figure 3).

In a related set of experiments conducted from undersaturation but involving $CaCl_2$ solutions, calcium-associated Th(IV) intrinsic colloids are the dominant mobile Th(IV) species above a pH (molal) of 10.5 (Altmaier et al. 2008). Concentrations of these colloids increase rapidly with increasing alkalinity. The

same trend is observed in the same study for Zr(IV) but begins at a pH (molal) of 9 to 9.5. The equilibration times for these tests were 7 to 198 days.

Intrinsic colloid data most relevant to the WIPP PA are data obtained from WIPP actinide solubility experiments(Borkowski et al. 2012; Reed et al. 2013a). Actinide solubilities have been measured in GWB and ERDA-6 that have been equilibrated for 2 to 6 years. The results of these experiments are summarized in Table 5-1.

The solubility of Th(IV) in carbonate-free and carbonate-containing GWB and ERDA-6 was measured as a function of pcH and time in a set of LANL experiments (Borkowski et al. 2012). After two years of equilibration, the concentrations of dissolved Th(IV) (6-7 × 10^{-7} M) were in the range of those reported in Altmaier et al. (2004), but the intrinsic colloid fraction was much lower, approximately 40%. To test whether the dissolved concentrations were at equilibrium, samples from the GWB solutions were re-examined after two more years. During this time, the total aqueous Th(IV) concentration decreased by more than an order of magnitude to 2 × 10^{-8} M at pcH 9.1 and to lower concentrations at pcH 9.6.

Long-term experiments relevant to actinides at other oxidation states have also shown measureable but low concentrations of intrinsic colloids in WIPP brines. Intrinsic colloids have been measured for Nd(III), Pu(III), and U(VI) at pcH values between 9.1 and 9.8 (Table 5-1).

Since the CCA other studies on intrinsic colloid formation for Pu(IV) and other actinides and actinide analogues have been reported in the literature. However, the solutions used in those experiments are either dilute compared to WIPP brines or the pcH is significantly different from the pcH expected for WIPP brines in contact with MgO. These studies include Neck and Kim (2001), Neck et al. (2002), Neck et al. (2003), Bitea et al. (2003), Vandenborre et al. (2008), and Powell et al. (2011).

Prediction of intrinsic Pu(IV) colloid stability has been advanced by Abdel-Fattah et al. (2013). These researchers calculated the Hamaker constant (~10^{-19} J) from optical parameters of PuO_2 calculated by Shi et al. (2010). The Hamaker constant is needed to calculate van der Waals interactions between colloids, including natural groundwater colloids, and between colloids and surfaces of the porous medium. Abdel-Fattah et al. (2013) used this constant to develop response surfaces as a function of pH and ionic strength to identify where energy barriers to aggregation are high between colloids of the same type, between colloids of different types, and between colloids and stationary surfaces. The results indicate that under WIPP conditions the energy barrier for intrinsic Pu(IV) colloid aggregation is very low.

Table 5-1. Concentrations of intrinsic colloids measured in WIPP brines in long-term experiments at anticipated pcH values

Actinide or Actinide Analogue	Intrinsic Colloid Concentration[a] (M)	Brine	Equilibration Time	Source
Nd(III)	4 × 10^{-9}	ERDA-6, pcH 9.14	2-6 years	Reed et al. (2013a)
Pu(III) [b]	4.8 × 10^{-9}	ERDA-6, pcH 9.1	6 years	Reed et al. (2013a)
Th(IV)	≤ 2 × 10^{-8}	GWB, pcH 9.1	4 years	Borkowski et al. (2012)
U(VI)	1 × 10^{-8}	ERDA-6, pcH 9.3-9.8	5 years	Reed et al. (2013a)

[a] Concentration of element in 2.5 to 10 nm size fraction
[b] In the presence of metallic iron

5.2.4 Analysis

5.2.4.1 Long term Th(IV) solubility experiments

Recent Th(IV) solubility data from four-year experiments on WIPP brines indicate that Th(IV) colloid concentrations continue to decrease significantly over time. The dissolved Th(IV) concentration measured

by Borkowski et al. (2012) after two years of equilibration was in the range of 6-7 × 10^{-7} M with intrinsic colloids accounting for approximately 40% of this concentration. After four years, the total dissolved Th(IV) concentration dropped more than an order of magnitude to 2 × 10^{-8} M (Borkowski et al. 2012). Because the 2 × 10^{-8} M measurement was performed without ultracentrifugation or ultrafiltration to separate the colloidal and truly dissolved Th(IV), the colloidal component is less than 2 × 10^{-8} M. This slow reduction in colloidal concentration is consistent with slow aggregation of Th(IV) colloids. It is also consistent with the formation of more crystalline forms of ThO_2.

Slow aggregation of Th(IV) intrinsic colloids in WIPP brines is consistent with energy barrier calculations for Pu(IV) intrinsic colloid aggregration (Abdel-Fattah et al. 2013). The energy barrier for intrinsic Pu(IV) colloid aggregation is very low for the ionic strength and pcH of WIPP brines. A low energy barrier implies that intrinsic colloids will sparingly resist aggregation. The reason slow aggregation is observed in the case of Pu(IV) and Th(IV) is attributed to very low concentrations. At low concentrations, aggregation is diffusion limited, i.e., rapid aggregation is prevented by low collision frequency (Abdel-Fattah et al. 2013).

5.2.4.2 Intrinsic Th(IV) colloid measurements of Altmaier et al. (2004)

The highest Th(IV) intrinsic colloid concentrations measured in the Altmaier et al. (2004) study were observed in carbonate-free NaCl or $MgCl_2$ solutions in one-day oversaturation experiments ($10^{-6.6}$ M to $10^{-5.6}$ M). These concentrations were considerably higher than those measured in their undersaturation experiments ($10^{-7.3}$ M to $10^{-6.3}$ M) that lasted 20 to 100 days (Altmaier et al. 2004). Data from Borkowski et al. (2012) from experiments using WIPP brines also show a significantly decreasing trend in concentration as a function of equilibration time. This trend and the findings of the Abdel-Fattah et al. (2013) study suggest that the intrinsic colloid concentrations measured in the Altmaier et al. (2004) study may have been unstable and slowly aggregating.

5.2.4.3 Th(IV) solubility for WIPP PA

For the CRA-2009 Performance Assessment Baseline Calculation (PABC) and CRA-2014 PA, Th(IV) concentration measurements from the non-centrifuged samples from Altmaier et al. (2004) are included in calculated solubility distributions but the lower measurements from ultracentrifuged samples are not (Xiong et al. 2011; Brush and Domski 2013c). The primary reason for this screening approach was to be consistent with the data set used for the original WIPP Th(IV) PABC model. Data for the original model was obtained using simple centrifugation and filtration methods.

For the CRA-2014 PA, CONCINT for Th(IV) was increased from 0 to 2 × 10^{-8} M based on the recommendations in Reed et al. (2013a); (Roselle 2013b). The contribution of Th(IV) intrinsic colloids, therefore, is at least partially double-counted in the CRA-2014 PA because it is also at least partially included in the solubility calculations. This approach, however, reduces the chances that predicted Th(IV) solubilities and Th(IV) releases are underestimated in the WIPP PA.

5.2.4.4 Effect of intrinsic colloids on calculated humic-bound and microbially-bound Th(IV)

As a component of total releases, intrinsic colloids do not play an important role in the WIPP PA. This result is consistent with the analyses for colloids at Yucca Mountain (Buck and Sassani 2007) where models that included intrinsic colloids and colloids from minerals derived from the natural and engineered system material (iron-oxide colloids) indicated that the mineral based colloids, not intrinsic colloids, tended to dominate colloid transport.

Intrinsic colloids, however, should nevertheless be appropriately represented in PA calculations. Intrinsic colloids should not be lumped with dissolved concentrations in the WIPP PA because intrinsic colloids

react and migrate differently than dissolved species and may also behave differently than other types of colloids (e.g., Abdel-Fattah et al. 2013). In addition, if actinides associated with intrinsic colloids are lumped into the dissolved fraction, calculations of the concentrations of other actinide components that are proportional to the dissolved concentration will be inflated. In the WIPP PA, concentrations of humic-bound and microbially-bound actinides are defined to be directly proportional to the dissolved concentration (Section 4.2); thus, overestimates of dissolved concentrations due to the inclusion of intrinsic colloids in the dissolved concentrations will result in overestimates of humic- and microbially-bound actinide concentrations.

5.2.4.5 Intrinsic colloids for An(III) and An(VI)

Results summarized in Reed et al. (2013a) show that intrinsic colloids of Nd(III), Pu(III), and U(VI) may also occur in brines. Though specific contributions of An(III) and An(VI) intrinsic colloids to total releases may be insignificant, their effects on truly dissolved concentrations, as in the case of Th(IV) and Pu(IV), may have significant effects on calculated humic-bound and microbially-bound actinides if intrinsic colloid contributions are not excluded from the dissolved concentration distributions (Section 5.2.4.4).

5.2.4.6 Potential effects of parsing dissolved and intrinsic colloid concentrations

The effects of excluding samples that have not undergone ultracentrifugation or ultrafiltration from the determination of WIPP PA dissolved concentrations are addressed here in a simple hypothetical example. It is supposed in this example that the truly dissolved concentration of Pu(IV) is one-third of the value currently being used in the WIPP PA. Because humic-bound and microbially-bound Pu(IV) are proportional to the dissolved concentration, each of these organic colloid component concentrations would therefore be reduced by one-third (provided initial concentrations were not limited by the maximum values of CAPHUM and CAPMIC). Reductions in humic-bound and microbially-bound Th(IV) would be much greater for much lower solubilities. For example, the EPA in its 2009 Technical Support Document (TSD) for Section 194.24 found that using a value of 8.49×10^{-10} M for dissolved Th(IV), based on ultracentrifuged solubility measurements from Altmaier et al. (2004), dropped the humic-bound and microbially-bound Th(IV) concentrations by more than an order of magnitude (Section 5.2.1).

The extent of defensible reduction in dissolved concentrations for Pu(IV) and other actinide species due to the exclusion of samples that have not been ultracentrifuged or ultrafiltered has not been investigated at this time. Currently available data have originated under different chemical conditions, different degrees of filtration and centrifugation, and different durations of equilibration, each of which have been shown to affect solubility measurements. However, the effects of the different conditions need to be better understood. For example, the Borkowski et al. (2012) study indicates that after two years of equilibration in WIPP brine no more than 40% of the measured solubility of Th(IV) was due to intrinsic colloids. These results are in contrast to the Altmaier et al. (2004) results which indicate that more than 99% of the measured Th(IV) solubility after 20 to 100 days in their salt solutions was due to intrinsic colloids. Whether these differences are due to equilibration time, different chemical conditions, different sampling procedures, other factors, or a combination of factors is not clear.

The difference of two orders of magnitude observed in the Altmaier et al. (2004) study of colloidal Th(IV) to dissolved Th(IV) is consistent with the difference in the two sets of compiled Th(IV) solubility log K values in Rand et al. (2008, Table VII-20). The first set of solubility log K values includes measurements obtained without sufficient centrifugation or filtration to remove intrinsic colloids, and the second set includes measurements obtained after ultracentrifugation or ultrafiltration. Log K values for the first set range from -6.8 to -5.7 while those for the second set range from -9.5 to -7.4. These data strongly support the idea that true Th(IV) solubility cannot be measured without ultracentrifugation, ultrafiltration, or some other means to remove the contribution of intrinsic colloids.

Any reduction of dissolved concentrations by removal of intrinsic colloids would need to be accompanied by a corresponding representation of intrinsic colloids. In the context of the WIPP PA, the CONCINT values for actinide species showing significant intrinsic colloid concentrations should be adjusted as appropriate.

The humic and microbial components of An(III) and An(IV) releases are particularly dominant in calculated WIPP releases (Figure 4-2). If the dissolved An(III) and An(IV) concentrations were to exclude intrinsic colloid contributions, the result would likely be a significant reduction in calculated overall WIPP releases.

5.2.5 Conclusions

5.2.5.1 A non-zero CONCINT value for Th(IV) intrinsic colloids should be used in the WIPP PA.

Data from the literature and from direct measurements on WIPP brines show that Th(IV) forms intrinsic colloids and that the concentrations of these colloids in alkaline brines are not an insignificant fraction of dissolved (<0.45 μm) thorium (Borkowski et al. 2012; Altmaier et al. 2004; Rand et al. 2008). In fact, numerous studies have found that the intrinsic colloid component may dominate dissolved Th(IV) concentrations (Altmaier et al. 2004; Rand et al. 2008). These intrinsic colloids may be unstable and may aggregate over time due to a low energy barrier to aggregation resulting from alkaline pH values and high ionic strength (Abdel-Fattah et al. 2013).

The concentration of Th(IV) associated with intrinsic colloids in WIPP brine experiments was measured to be approximately 40% of the 6-7 × 10^{-7} M total dissolved concentration after two years of equilibration (Borkowski et al. 2012). After four years of equilibration the total dissolved Th(IV) concentration dropped to 2 × 10^{-8} M (Borkowski et al. 2012). This total concentration is less than 10% of both the colloidal Th(IV) and truly dissolved Th(IV) concentrations from two years prior. Thus, both the colloid and dissolved fractions of Th(IV) dropped markedly.

The CONCINT value of 2 × 10^{-8} M used in the CRA-2014 PA for Th(IV) is based on the lower four-year measurement. A conservative approach for determining the CONCINT value for Th(IV) would be to choose the maximum value of Th(IV) associated with intrinsic colloids in the two-year Borkowski et al. (2012) experiments (~3 × 10^{-7} M). This value would be approximately consistent with the range of concentrations measured in the Altmaier et al. (2004) undersaturation experiments. Using this more conservative value would require positing, if reasonable, the potential relevance of shorter time frames. To further support or improve the recommended CONCINT value, confirmatory data are needed; however, reduced uncertainty in this value would not likely have a considerable effect on calculated WIPP releases due to low concentrations relative to releases owing to organic colloids.

5.2.5.2 The set of solubility data used to determine dissolved concentration distributions for the WIPP PA model should exclude solubility measurements known or likely to contain large contributions from intrinsic colloids.

Including solubility measurements containing significant contributions from intrinsic colloids in the WIPP PA solubility distributions is conservative for the calculation of dissolved actinide concentrations. At the same time, this practice may also significantly inflate WIPP PA calculations of humic-bound and microbially-bound actinides. The concentrations of organically-bound actinide components are defined to be directly proportional to dissolved concentrations in the WIPP PA (except when they are calculated to exceed the CAPHUM and CAPMIC values, at which point they are set at the CAPHUM and CAPMIC values). The concentration of humic-bound actinides calculated in the WIPP PA should depend only on the non-colloidal dissolved concentration, as represented in Equations 1 and 2 of Section 4.2. An analogous relationship is established for microbial colloids in the WIPP PA. For these reasons, the

dissolved actinide concentrations determined in the WIPP PA should represent as best as possible the true non-colloidal fraction.

5.2.5.3 CONCINT values should be used for each actinide species that forms significant concentrations of intrinsic colloids in WIPP brines.

Because intrinsic colloids have been observed for actinide species other than Pu(IV), CONCINT values should be used for each of these species. This has been done for the CRA-2014 PA (Section 5.2.2). Solubility experiments using WIPP brines at anticipated pcH values followed by ultracentrifugation or ultrafiltration are useful in determining the CONCINT values. Currently available data for An(III) and U(VI) in WIPP brines are summarized in Reed et al. (2013). Except for U(VI), whose dissolved concentration is fixed in the WIPP PA, this information could potentially justify reducing the dissolved concentrations that are used to calculate actinide concentrations bound to humic and microbial colloids.

Concentrations of intrinsic colloids measured in both short-term and long-term experiments can be used to determine the likely and potential intrinsic colloid fractions in the solubility measurements currently included in the WIPP PA solubility data sets. This information would help to determine whether solubility measurements from past experiments on samples that have not undergone ultracentrifugation or ultrafiltration should be excluded from solubility distributions due to intrinsic colloids. Not only would measurements of intrinsic colloid concentrations be obtained from these experiments, but measurements of the truly dissolved concentrations would be obtained. These truly dissolved concentration measurements would likely be lower than measurements from samples that are not ultracentrifuged or ultrafiltrated and, if used in solubility determinations in place of measurements from ultracentrifuged or ultrafiltrated samples, would likely improve the solubility distributions used to determine the dissolved concentrations for the WIPP PA. This improvement would likely reduce the mean dissolved concentrations for a subset of the actinides and reduce the likelihood that concentrations of actinides bound to humic and microbial colloids would be overestimated in the WIPP PA.

5.3 Humic Substance Colloids

5.3.1 EPA Comments

In its CRA-2009 TSD, the EPA noted that, based on the actinide solubilities used for CCA PA, the humic substances colloids and microbial colloids were the largest contributors to mobile actinides in the source term (EPA 2010, Table 8-1 and discussion).

5.3.2 Current PA Representation

The current PA representation of the humic substance colloid model is explained in detail in Section 4.2.3. The humic colloid model is more involved than the models for intrinsic and mineral fragment colloids because the concentration of actinides associated with humic substances is a function of the modeled dissolved concentration. At low values of dissolved actinide concentrations, the actinide concentration associated with humic substances is proportional to the dissolved concentration and is calculated by multiplying the dissolved concentration by a proportionality constant, PHUMSIM or PHUMCIM, depending on whether the brine is from the Salado or the Castile, respectively (Section 4.2). However, if this product exceeds the maximum actinide concentrations allowed to be bound to humic colloids, defined by the model parameter CAPHUM, then the CAPHUM value is used in place of the product. The established value for CAPHUM, 1.1×10^{-5} M, is based on a site-binding capacity of 5.56 meq g^{-1} and a maximum humic colloid concentration of 2.0 mg L^{-1}.

5.3.3 Literature Review

Since the CCA a number of studies have been published that address the stability of humic substances in brines and the effects of ionic strength and pH on the complexation of dissolved ions by aqueous humic substances. The most pertinent of these publications are mentioned here.

Wall and Choppin (2003) studied the solubility of humic acid in solution as a function of solution composition. The results indicate that coagulation, to a first approximation, is consistent with DLVO theory. Coagulation increased with increasing ionic strength, increasing cationic charge, and decreasing size of hydrated ions in the double layer.

Building on this work, Wall and Mathews (2005) studied the stability of humic acids in 95% GWB and 95% ERDA-6 in the presence and absence of MgO. This study showed that humic acids are not highly stable in the presence of MgO and that their concentrations will decrease below detection within 60 days of MgO addition. This study is examined in Section 5.3.4.1.

The aqueous stability of humic substances and mineral fragments may be enhanced by the attachment of these colloids to one another. Hu et al. (2010) studied the stability of magnetite nanoparticles (58.0 ± 0.3 nm) in the presence and absence of humic acids over broad ranges of pH (3 to 10) and ionic strength (0.001 to 0.1 M NaCl). The results show that humic acid, depending on pH and ionic strength, can act to stabilize or destabilize the magnetite particles. In the solutions with the highest ionic strength, humic acid at a concentration of 2 mg L^{-1} significantly stabilized the magnetite particles. These observations agree well with the DLVO calculations also presented in the paper. Similar trends are observed for fulvic acid in the presence of iron oxide nanoparticles (Palomino and Stoll 2013).

Studies since the CCA also include those pertaining to the complexation of metals and actinides to aqueous humic substances. Of particular note, complexation of Th(IV) with humic acid was measured over a broad range of pH but at low ionic strength (Reiller et al. 2008). In addition, laboratory studies have continued on humic acid complexation of actinides and lanthanides, particularly Am(III), Eu(III), and U(VI), but at low ionic strength (Sakuragi et al. 2005; Moser et al. 2012). Only a few studies published since the CCA involve humic and fulvic acid complexation of actinides and other metals in brine. They include the complexation of 10^{-6} M Ca with Aldrich humic acid in NaCl solutions up to 5 molal over a pcH range of 4.7 to 9.0 (Laszak and Choppin 2001), and complexation of 10^{-9} M Am(III) with humic acid from Lake Bradford in Florida and fulvic acid from Suwannee River in NaCl solutions up to 5 molal at a pcH of 5.0 to 5.1 (Wall et al. 2002). No studies of humic complexation with metals or actinides were found that involve high concentrations of Ca or Mg comparable to the Ca and Mg concentrations in WIPP brines.

5.3.4 Analysis

5.3.4.1 Humic colloid stability in WIPP brines

Wall and Mathews (2005) studied the stability of humic acid in 95% GWB and 95% ERDA-6 in the presence and absence of MgO. Results are shown in Table 5-2 and Figure 5-2. Humic acid was found to be stable in those solutions at a concentration of approximately 30 mg L^{-1} in the absence of MgO. Addition of MgO, however, destabilized the humic acids and their concentrations fell below detection within 60 days. The detection limit in these experiments was not reported. Based on the error bars in the figures, it was likely greater than 1 mg L^{-1}.

Without the MgO addition, the average pH values in the solutions were in the range of 7 to 8. In the presence of MgO, the pH was generally higher, in the range of 8.1 to 12.8. Because WIPP waste forms are surrounded by MgO, these results suggest that humic substance colloids may be unstable in WIPP source-term brines. However, further study is needed to confirm this because fulvic acids were not

included in this study and detection limits were not low enough to rule out potentially significant concentrations of humic acids.

Table 5-2. Average pH and 60-day humic acid concentration in presence and absence of MgO in Wall and Mathews (2005) study

Mineral Phase	Solution	Humic Acid (mg L^{-1})	pH[c]
None	Deionized water	290 ± 10	NR[e]
	95% ERDA-6	31 ± 4	7.92 ± 0.03
	95% GWB	30 ± 4	7.08 ± 0.08
Fisher MgO[a]	Deionized water	ND[d]	11.2 ± 0.5
	95% ERDA-6	ND	10.7 ± 0.1
	95% GWB	ND	8.1 ± 0.2
Premier MgO[b]	Deionized water	ND	12.8 ± 0.1
	95% ERDA-6	ND	12.1 ± 0.1
	95% GWB	ND	8.4 ± 0.1

[a] 97.0% MgO
[b] 87 – 89% MgO (impurities: monticellite, forsterite, lime, and spinel)
[c] For solutions containing MgO, pH was only reported for 2.4 g g^{-1} liquid:solid ratio
[d] Below detection for both liquid:solid ratios studied (2.4 and 10.0 g g^{-1})
[e] Not reported

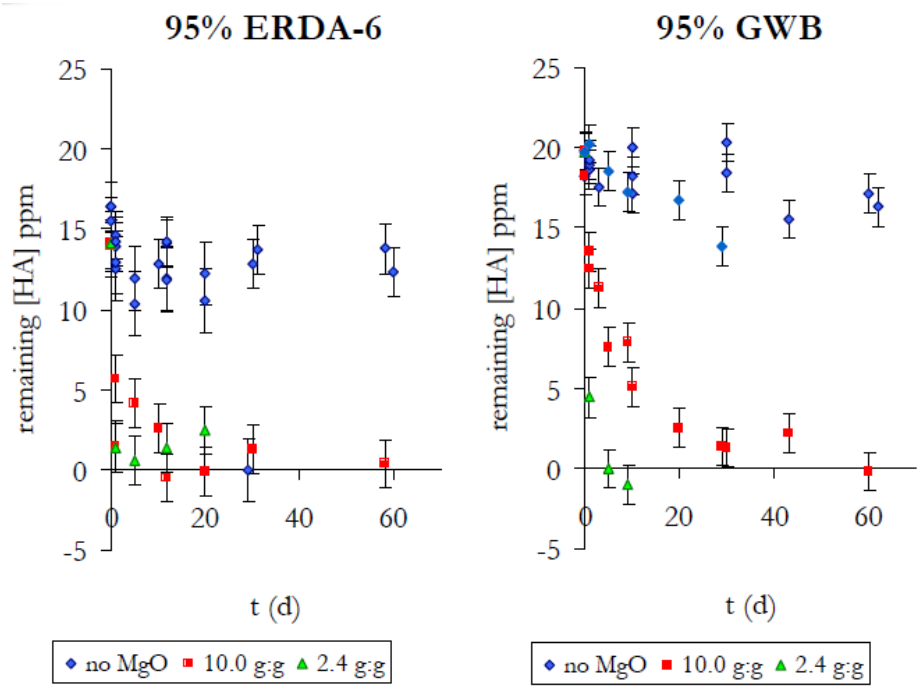

Figure 5-2. Humic acid concentration over time for different liquid:solid ratios for both 95% GWB and 95% ERDA-6 (graphic from Wall and Mathews (2003)).

5.3.4.2 PHUMSIM and PHUMCIM for An(III), An(V), and An(VI)

The PHUMSIM and PHUMCIM proportionality constants for An(III), An(V), and An(VI) species were derived as explained in Section 4.2.3. PHUMSIM and PHUMCIM are distribution coefficients, i.e., calculated values of $[\mathrm{AnHS}]/[\mathrm{An}]$. The calculations presented in Table 4-3 verify that the data in that table and the following parameters were used to calculate PHUMSIM and PHUMCIM for An(III), An(V), and An(VI):

- Humic complexation constants, $\beta_{1:\mathrm{An}}$, for Am(III), Np(V), and U(VI)
- Humic-Ca/humic-Mg complexation constant, $\beta_{1:\mathrm{CaMg}}$
- Humic binding site concentration, $[\mathrm{HS}_{\mathrm{tot}}]$
- Combined Ca and Mg concentrations in GWB and ERDA-6, $[\mathrm{Ca}+\mathrm{Mg}]$
- Total aqueous non-colloidal concentrations of Am(III), Np(V), and U(VI), $[\mathrm{An}]$

The $\beta_{1:\mathrm{An}}$ values for Am(III) and U(VI) came from experiments involving humic and fulvic acids performed in 6 molal NaCl solutions at pH 6 (DOE 1996, SOTERM.6.3.3.1). (Note: There is a possible error in the $\beta_{1:\mathrm{An}}$ values used for U(VI). This is addressed in Section 5.3.4.3). The $\beta_{1:\mathrm{An}}$ value for Np(V) was obtained from a study using Gorleben humic acid in a pH 9 solution in 0.1 M $NaClO_4$ (Kim and Sekine 1991). The $\beta_{1:\mathrm{CaMg}}$ value came from experiments that involved humic and fulvic acids performed under acidic conditions in 0.1 M $NaClO_4$ (Section 4.2.3). The value of $[\mathrm{HS}_{\mathrm{tot}}]$ assumes a 2.0 mg L^{-1} humic colloid concentration for the WIPP brines, and the total aqueous non-colloidal concentrations of the actinides are those assumed for WIPP brines in the presence of MgO, as defined in Papenguth (1996, Tables 1a and 1b) and shown in Table 4-3.

When direct measurements of partitioning are unavailable in the solutions of interest, they can only be approximated from known relationships. As noted above, the PHUMSIM and PHUMCIM values use several inputs that were derived from solutions that do not have an alkaline pH (except for Np(IV)) or high concentrations of divalent cations, as are expected for WIPP brines in contact with MgO backfill. For three of these inputs, $\beta_{1:\mathrm{An}}$, $\beta_{1:\mathrm{CaMg}}$, and $[\mathrm{HS}_{\mathrm{tot}}]$, values are conservatively chosen.

Conservative values of $[\mathrm{An}]$ were also used in the calculation of PHUMSIM and PHUMCIM. At low loadings of humic complexation sites, the values of distribution coefficients are unaffected by $[\mathrm{An}]$. At high loadings, increased $[\mathrm{An}]$ will reduce distribution coefficients because the limited availability of complexation sites will limit the increase in $[\mathrm{AnHS}]$, as defined in Eq. 7. For example, the 10^{-5} M concentration of U(VI) used in the calculation of An(VI) PHUMSIM and PHUMCIM is conservative because it is two orders of magnitude lower than the CRA-2014 PA solubility of 10^{-3} M, and high loading of complexation sites by U(VI) is expected for this range of U(VI) concentration for the assumed value of $[\mathrm{HS}_{\mathrm{tot}}]$.

The combined effect of using conservative values for $\beta_{1:\mathrm{An}}$, $\beta_{1:\mathrm{CaMg}}$, $[\mathrm{HS}_{\mathrm{tot}}]$, and $[\mathrm{An}]$ is difficult to assess without knowledge of the degree to which each value is conservative. The results of a simple one-off sensitivity study are presented below.

Effect of $[\mathrm{HS}_{\mathrm{tot}}]$

A lower value of $[\mathrm{HS}_{\mathrm{tot}}]$ results in proportionally lower PHUMSIM and PHUMCIM values. This relationship is easily shown by Eq. 7. Thus, the proportionality constants are directly proportional to the

humic colloid concentration, which, as discussed in Section 5.3.4.1, may be much lower than the 2.0 mg L^{-1} value assumed for it.

Effect of $\beta_{1:CaMg}$

The value of $\beta_{1:CaMg}$ has nearly the same magnitude of effect as $[HS_{tot}]$ but in the inverse direction. Its effect is large because the value of the product $\beta_{1:CaMg}$ $[Ca + Mg]$ is generally much larger than the sum of $\beta_{1:An}[An]$ + 1 in the denominator of Eq. 7 for the modeled actinides, implying the former will dominate the latter in the denominator. Its effect in the case of U(VI) in the Castile brine is diminished somewhat due to the order of magnitude lower $[Ca + Mg]$ concentration in the Castile and the relatively high $\beta_{1:An}[An]$ product for U(VI). However, as shown in Section 5.3.4.5, humic-bound U(VI) is usually limited to CAPHUM.

Effect of $\beta_{1:An}$

In the calculations for Am(III) and Np(V) in both brines and for U(VI) in the Salado brine, a reduction in the value of $\beta_{1:An}$ causes nearly the same proportional change to PHUMSIM and PHUMCIM. This parameter is in both the numerator and denominator of Eq. 7. It has little effect in the denominator when $\beta_{1:An}[An]$ is small relative to $\beta_{1:CaMg}$ $[Ca + Mg] + 1$. For U(VI) in Castile brine, this is not the case, and as a result the effect on PHUMCIM is diminished for U(VI). However, as shown in Section 5.3.4.5, humic-bound U(VI) is usually limited to CAPHUM.

Effect of $[An]$

For An(V), uncertainty in the value of $[An]$ has a negligible effect on $[AnHS]/[An]$ because the values of $[An]$ and $\beta_{1:An}$ for An(V) are sufficiently low that the distribution of An(V) between dissolved and humic-bound phases is essentially linear.

For U(VI), the CRA-2014 PA 10^{-3} M concentration is much higher than the 10^{-5} M concentration used to calculate the currently used U(VI) PHUMSIM and PHUMCIM values (Table 4-3). Use of the 10^{-3} M value in place of the 10^{-5} M value would cause $[AnHS]/[An]$ to decrease significantly, as shown in Table 5-3. To be consistent with a 10^{-3} M dissolved concentration, PHUMSIM and PHUMCIM would need to be more than an order of magnitude lower than current values. This inherent conservatism in the current values, however, does not propagate into the humic-bound U(VI) concentration of the WIPP PA because the calculations based on the current PHUMSIM and PHUMCIM values and the 10^{-3} M solubility exceed CAPHUM (Section 5.3.4.5).

Table 5-3. Calculated values of humic-bound actinide concentrations $[AnHS]$ and $[AnHS]/[An]$ using CRA-2014 PA solubility (estimated using minimum brine volume) combined with constants from Papenguth (1996, Tables 1a, 1b, and 3)

Formation	Actinide	$[An]$ (M)	Humic Substance	$[HS_{tot}]$ (M)	log $\beta_{1:An}$	$[AnHS]$ (M)	$[AnHS]/[An]$
Salado	U(VI)	1.00E-03	HAal-LBr	9.3E-06	5.91	1.2E-06	0.0087
			HAal-Gor	1.1E-05	5.35	4.2E-07	0.0086
			FA-Suw	1.1E-05	4.60	8.0E-08	0.0047
	Np(V)	2.77E-07	HAal-Gor	1.1E-05	3.67	2.5E-10	9.1E-04
	Am(III)	2.59E-06	HAal-LBr	9.3E-06	6.09	8.3E-07	0.20
			HAal-Gor	1.1E-05	6.02	8.3E-07	0.20
			FA-Suw	1.1E-05	4.60	3.5E-08	0.0080
Castile	U(VI)	1.00E-03	HAal-LBr	9.3E-06	5.91	5.1E-06	0.009
			HAal-Gor	1.1E-05	5.35	2.7E-06	0.010
			FA-Suw	1.1E-05	4.60	6.2E-07	0.010
	Np(V)	8.76E-07	HAal-Gor	1.1E-05	3.67	6.5E-09	7.4E-03
	Am(III)	1.48E-06	HAal-LBr	9.3E-06	6.09	6.5E-07	1.33
			HAal-Gor	1.1E-05	6.02	6.5E-07	1.36
			FA-Suw	1.1E-05	4.60	2.7E-08	0.065

For An(III), the effect of using the baseline $[An]$ instead of the $[An]$ values from Papenguth (1996, Tables 1a and 1b) on the calculation of $[AnHS]/[An]$ would be small (Table 5-3). However, because An(III) is represented by an uncertainty distribution that varies over more than six orders of magnitude, the effect would be large for sampled values of $[An]$ that are in the high end of the distribution. Thus, the degree of conservatism inherent in the An(III) $[AnHS]/[An]$ values due to the effect of $[An]$ would be small or negligible for sampled $[An]$ values less than the baseline value but would be quite large for sampled $[An]$ values in the upper end of the solubility distribution. Propagation of very large calculated values of $[AnHS]$ based on the currently used PHUMSIM and PHUMCIM values is prevented by CAPHUM.

Effect of Multiple Sources of Conservatism

The conservatisms in the values chosen for $\beta_{1:An}$, $\beta_{1:CaMg}$, $[HS_{tot}]$, and $[An]$ propagate multiplicatively into the calculation of PHUMSIM and PHUMCIM. For example, if the values for $\beta_{1:An}$, $\beta_{1:CaMg}$, and $[HS_{tot}]$ are each conservative by a factor of 2, then based on the sensitivity analysis above, the PHUMSIM and PHUMCIM values would be conservative by nearly a factor of 8 (i.e., 2×2×2) for all but PHUMCIM for U(VI). Actual quantitative propagation of such a scenario shows that indeed PHUMSIM for An(III), An(V), and An(VI) and PHUMCIM for An(III) and An(V) would decrease by factors between 7 and 8 in this example, as shown in Table 5-4. Calculated $[AnHS]/[An]$ values for An(VI) in Castile brine associated with HAal-LBr and HAal-Gor (Table 4-3) for the same scenario would decrease by factors of 4.5 and 6.1, respectively.

Table 5-4. Calculated values of humic-bound actinide concentrations $[AnHS]$ and $[AnHS]/[An]$ using halved values for $\beta_{1:An}$ and $[HS_{tot}]$ and a doubled value for $\beta_{1:CaMg}$ compared to Table 4-3

Formation	Actinide	$[An]$ (M)	Humic Substance	$[HS_{tot}]$ (M)	log $\beta_{1:An}$	$[AnHS]$ (M)	$[AnHS]/[An]$
Salado	U(VI)	1.00E-05	HAal-LBr	4.7E-06	5.61	1.7E-07	0.017
			HAal-Gor	5.4E-06	5.05	5.5E-08	0.005
			FA-Suw	5.6E-06	4.30	1.0E-08	0.0010
	Np(V)	2.64 E-06	HAal-Gor	5.4E-06	3.37	3.0E-10	1.2E-04
	Am(III)	4.39 E-06	HAal-LBr	4.7E-06	5.79	1.1E-07	0.026
			HAal-Gor	5.4E-06	5.72	1.1E-07	0.025
			FA-Suw	5.6E-06	4.30	4.4E-09	0.0010
Castile	U(VI)	1.00E-05	HAal-LBr	4.7E-06	5.61	1.1E-06	0.114
			HAal-Gor	5.4E-06	5.05	4.4E-07	0.044
			FA-Suw	5.6E-06	4.30	8.7E-08	0.009
	Np(V)	2.53 E-06	HAal-Gor	5.4E-06	3.37	2.5E-09	1.0E-03
	Am(III)	4.12 E-07	HAal-LBr	4.7E-06	5.61	9.2E-08	0.22
			HAal-Gor	5.4E-06	5.05	9.1E-08	0.22
			FA-Suw	5.6E-06	4.30	3.6E-09	0.009

Greater decreases in calculated $[AnHS]/[An]$ values are possible due to the potential for greater factors of conservatism in the $\beta_{1:An}$, $\beta_{1:CaMg}$, $[HS_{tot}]$, and $[An]$ values selected for the PHUMSIM and PHUMCIM calculations. While the potential for a very low value for $[HS_{tot}]$ has been presented in Section 5.3.4.1, the degree of conservatism in the values of $\beta_{1:An}$ and $\beta_{1:CaMg}$ are not explored in this report. Values of these parameters under conditions of high pH and high concentrations of Ca and Mg have not been measured, so evaluating the degree of conservatism in these values would be conjecture and would not permit the derivation of new, easily-defended conservative values. Another way to evaluate the degree of conservatism in these inputs would be to compare the resulting PHUMSIM and PHUMCIM values with directly observed partitioning of Am(III), Np(V), and U(VI) with aqueous humic substances in WIPP brines in the presence of MgO if there were data for this comparison.

5.3.4.3 PHUMSIM and PHUMCIM values for U(VI)

There is a discrepancy in the U(VI) log $\beta_{1:An}$ values used to calculate PHUMSIM and PHUMCIM for U(VI) (shown in Table 4-3) and those reported in Labonne-Wall et al. (1999). The values reported in Labonne-Wall et al. (1999, Table 5) at pH 6.5, 6.6, and 6.5 in 6 m NaCl are 8.2 ± 0.5, 8.5 ± 0.1, and 7.8 ± 0.1 for HAal-LBr, HAal-Gor, and FA-Suw, respectively. Those presented in Papenguth (1996) and used to calculate PHUMSIM and PHUMCIM are much lower (5.91, 5.35, and 4.60).

Using the Labonne-Wall et al. (1999) log $\beta_{1:An}$ values in place of the Papenguth (1996) values in the Table 4-3 calculations would result in much higher $[AnHS]/[An]$ values, as shown in Table 5-5. Note that the values of $[AnHS]$ are nearly equal to $[HS_{tot}]$, i.e., CAPHUM. However, as shown in Sections 5.3.4.2 and 5.3.4.5 the values of humic-bound U(VI) calculated from the currently used PHUMSIM, PHUMCIM, and solubility values for U(VI) already exceed CAPHUM and are therefore ignored in the WIPP PA.

Table 5-5. Calculated values of humic-bound U(VI) concentrations [AnHS] and [AnHS]/[An] using the U(VI) complexation constants of Labonne-Wall et al. (1999)

Formation	Actinide	[An] (M)	Humic Substance	$[HS_{tot}]$ (M)	log $\beta_{1:An}$	[AnHS] (M)	[AnHS]/[An]
Salado	U(VI)	1.00E-05	HAal-LBr	9.3E-06	8.2	9.0E-06	0.90
			HAal-Gor	1.1E-05	8.5	1.1E-05	1.06
			FA-Suw	1.1E-05	7.8	1.0E-05	1.02
Castile	U(VI)	1.00E-05	HAal-LBr	9.3E-06	8.2	9.3E-06	0.93
			HAal-Gor	1.1E-05	8.5	1.1E-05	1.07
			FA-Suw	1.1E-05	7.8	1.1E-05	1.10

5.3.4.4 PHUMSIM and PHUMCIM values for An(IV)

The value for PHUMSIM and PHUMCIM for An(IV) is set at 6.3. This value is based on measurements of the distribution of Th(IV) in seawater between colloidal size particles (those particles passing through a 0.4 µm filter but retained by a 10K Dalton hollow fiber cross-flow ultrafiltration membrane) and smaller species (those passing through the 10K Dalton membrane), as reported in Baskaran et al. (1992).

Fourteen samples were collected and analyzed for dissolved and colloidal concentrations of Th(IV). A histogram of the [AnHS]/[An] ratios in these samples, calculated by dividing the $f_{c/d}$ values by the f_d values in Table 4 of the publication, are shown in Figure 5-3. These data indicate that the PHUMSIM and PHUMCIM value of 6.3 set for An(IV) is considerably higher than the [AnHS]/[An] ratios observed in seawater. Baskaran et al. (1992) measured dissolved organic carbon in two of the samples (90G14-5 and 90G14-10) and found them to have concentrations of 1.59 and 1.10 mg C L^{-1}, which are near the 2 mg L^{-1} concentration of humic colloids assumed for WIPP brines.

The partitioning of Th(IV) in seawater is expected to be a conservative analogue for the partitioning that would likely occur in WIPP brines in the presence of MgO. Seawater has a lower salinity than WIPP brines. The ionic strength of seawater is approximately 0.7 M, owing largely to Na and Cl. Seawater Ca and Mg concentrations are approximately 0.01 and 0.05 M, respectively. Although the Ca concentrations in WIPP brines equilibrated with MgO are in the same range as seawater, Mg concentrations are much higher (0.16 and 0.58 M, respectively, for ERDA-6 and GWB, Table 3-1). The higher Mg concentrations, pH, and reduced stability of humic colloids in WIPP brines equilibrated with MgO (Section 5.3.4.1) are expected to reduce the [AnHS]/[An] ratio of An(IV) compared to what is observed in seawater.

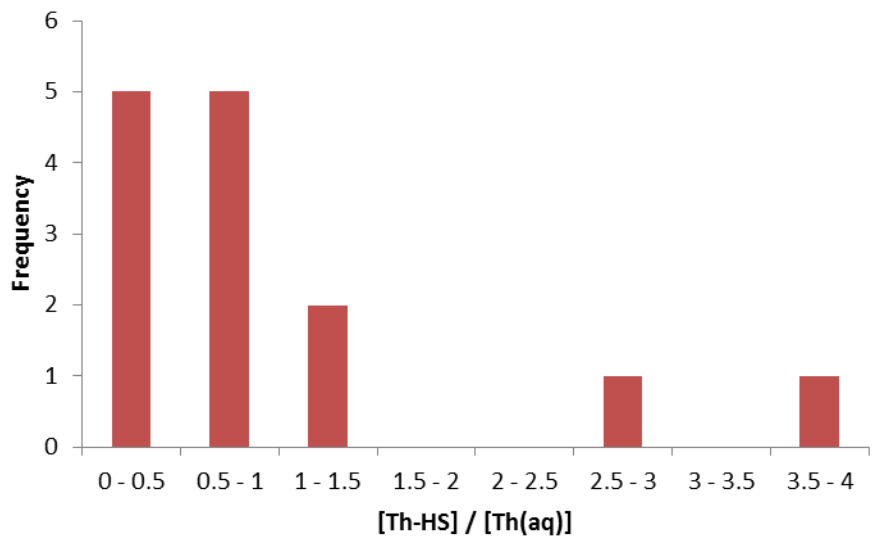

Figure 5-3. Histogram of measured [AnHS]/[An] ratios for Th(IV) in seawater (calculated from Table 4 of Baskaran et al. 1992).

5.3.4.5 CAPHUM

The CAPHUM value of 1.1×10^{-5} M, determined by multiplying the concentration of humic colloids (2 mg L^{-1}) by the maximum measured site binding capacity (5.56 meq g^{-1}), ensures that the humic-bound concentration of an actinide species does not exceed the capacity of available humic colloids. This value is conservative because

- the concentration of humic substances in WIPP brines in the presence of MgO is likely to be much lower than 2 mg L^{-1} (Section 5.3.4.1),
- the selected site binding capacity of 5.56 meq g^{-1} is the highest value measured among the three humic substances studied for the CCA (HAal-LBr, HAal-Gor, and FA-Suw),
- the site binding capacity assumes 1:1 binding of monovalent actinides,
- full loading of all binding sites by actinides will not occur due to competition of non-actinides for binding sites, and
- the competition between each actinide for binding sites is ignored in the humic colloid model, allowing the total effective loading for five actinides to increase above a total of 1.1×10^{-5} M.

Because the stability of humic colloids in WIPP brines in contact with MgO is likely much lower than 2 mg L^{-1} (Section 5.3.4.1), the bulk of the conservatism in CAPHUM is likely due to the humic colloid concentration assumption. The remaining four assumptions by themselves could also cause considerable overestimation in CAPHUM depending on the number of actinides that have humic-bound concentrations that approach, or are limited by, CAPHUM. However, multiple actinides with humic-bound concentrations near or equal to CAPHUM are likely to occur only in a small fraction of the simulations. Based on the baseline values of actinide solubility in the CRA-2014, only the concentration of humic-bound U(VI) will be limited by CAPHUM in the majority of the simulations (Table 5-6).

Table 5-6. Baseline humic-bound actinide concentrations consistent with CRA-2014 PA actinide solubilities

Actinide Species	Baseline Solubility (M) in CRA-2014 PA[a]		PHUMSIM	PHUMCIM	Baseline Humic-Bound Concentration (M)	
	Salado	Castile			Salado	Castile
An(III)	2.59E-06	1.48E-06	0.19	1.37[b]	4.9E-07	2.0E-06
An(IV)	6.05E-08	7.02E-08	6.3	6.3	3.8E-07	4.4E-07
An(V)	2.77E-07	8.76E-07	9.1E-04	7.4E-03	2.5E-10	6.5E-09
An(VI)	1.00E-03	1.00E-03	0.12	0.51	1.1E-05[c]	1.1E-05[c]

[a] Source: Brush and Domski (2013a); Brush and Domski (2013b)
[b] Median value (DOE 1996, Appendix SOTERM, Table SOTERM-14)
[c] Limited by CAPHUM

5.3.5 Conclusions

5.3.5.1 The stability of humic and fulvic acids in WIPP brines in the presence of MgO and inorganic colloids requires further laboratory study.

The laboratory experiments of Wall and Mathews (2005) indicate that humic acids are likely unstable in WIPP brines in the presence of MgO. To rule out the stability of humic colloids under WIPP conditions, however, more definitive data are needed. Fulvic acids were not included in the analyses. In addition, the detection limit for humic acid was not reported in the publication and was likely greater than 1 mg L^{-1} based on the error bars in the data presented.

It is possible that organic substances sorbed to inorganic phases may produce stable and significant colloid concentrations under conditions that may not support significant concentrations of humic and inorganic colloids by themselves (Palomino and Stoll 2013; Borgnino 2013; Hu et al. 2010). This possibility, which is not specifically addressed in the WIPP colloid model, should be investigated in the laboratory for solutions relevant to WIPP conditions.

5.3.5.2 If humic substances are found to be stable at potentially significant concentrations in WIPP brines in the presence of MgO, laboratory studies will be needed to directly measure the association of An(III) and An(IV) actinides with humic colloids under these same conditions.

If it is found that significant concentrations of humic colloidal material are likely to be stable in WIPP brines in contact with MgO, it will be important to study the effects of WIPP brines and MgO on the stability constants. An(III) and An(IV) produces the bulk of the releases in the WIPP PA; therefore, the complexation of An(III) and An(IV) with colloidal humic matter is of highest priority. To date, no laboratory studies of actinide-humic complexation have been performed in WIPP brines in the presence of MgO. Because pcH and the concentrations of Ca and Mg strongly affect actinide-humic complexation, studies are needed to measure this complexation under WIPP conditions.

5.3.5.3 To be consistent with the methodology developed for the CCA, PHUMSIM and PHUMCIM for U(VI) should be calculated using the log $\beta_{1:An}$ values of Labonne-Wall et al. (1999) and the established dissolved U(VI) concentration of 10^{-3} M.

Using the U(VI) log $\beta_{1:An}$ values of Labonne-Wall et al. (1999) and the 10^{-3} M dissolved concentration of U(VI) established for WIPP PA calculations, the value of $[AnHS]$ would be calculated to be equal to the site binding capacity $[HS_{tot}]$ (which is equal to CAPHUM). This must be so because the high values of

$\beta_{1:An}$ and $[An]$ cause $\beta_{1:An}[An] \gg \beta_{1:CaMg}[Ca + Mg] + 1$, which causes the denominator of Eq. 7 to cancel the $\beta_{1:An}[An]$ product in the numerator. Given these revised inputs of log $\beta_{1:An}$ and $[An]$, the value of the U(VI) PHUMSIM and PHUMCIM would be 0.011 and equal to $[HS_{tot}]/[An]$. This value multiplied by $[An]$, as in Eq. 1 and 2, would produce a value of $[AnHS]$ that is equal to CAPHUM. Because the WIPP PA model currently predicts that the $[AnHS]$ value for U(VI) is equal to CAPHUM, this change would not alter the total mobilized U(VI) concentrations predicted in the WIPP PA.

5.4 Microbial Colloids

5.4.1 EPA Comments

In its CRA-2009 TSD, the EPA noted that, based on the actinide solubilities used for the CCA PA, the humic substances colloids and microbial colloids were the largest contributors to mobile actinides in the source term (EPA 2010, Table 8-1 and discussion).

5.4.2 Current PA Representation

The microbial colloid model implemented in the WIPP PA is described in Section 4.2.4. The concentration of actinides associated with microbial colloids is calculated in the same manner as that associated with humic colloids. A proportionality constant, in this case PROPMIC, is multiplied by the dissolved actinide concentration $[An]$ to obtain the microbe-bound actinide concentration, and if this product exceeds a maximum value, in this case CAPMIC, the microbial actinide component is limited to CAPMIC.

In the CRA-2014 PA, the same parameters and equations were used to calculate microbially-bound actinide concentrations, but the values for PROPMIC and CAPMIC were updated as shown in Table 5-7 (Roselle 2013b). These values are recommended by Reed et al. (2013a, Table 3) for the far field where bacteria are expected to predominate over archaea. Because the WIPP PA model can only simulate a single set of PROPMIC and CAPMIC values, the more conservative values for bacteria were selected over the values for the near field where archaea are expected to predominate (Roselle 2013b; Reed et al. 2013a).

Table 5-7. PROPMIC and CAPMIC values used in the CRA-2014 PA (Roselle 2013b)

Radioelement	PROPMIC	CAPMIC (M)
Th	1.76	2.3×10^{-6}
U	1.76	2.3×10^{-6}
Np	1.76	2.3×10^{-6}
Pu	1.76	2.3×10^{-6}
Am	0.32	3.1×10^{-8}

5.4.3 Literature Review

A review of the literature relevant to the WIPP microbial colloid model has recently been performed and documented in Reed et al. (2013a) and therefore is not repeated here. In that report, studies involving high-ionic-strength water are cited, including McGenity et al. (2000), Gruber et al. (2004), Ams et al. (2013), Swanson et al. (2012), Swanson et al. (2013), and Swanson and Simmons (2013). The studies pertain to the types of microbes expected in the WIPP environment, the potential attachment of actinides to those microbes, and the abundance of those microbes. Several studies conducted under low-ionic-strength conditions are also identified in the report.

In addition to the literature review, the Reed et al. (2013a) report examines the WIPP microbial colloid model in light of recent data and recommends specific changes to improve the model. The Reed et al. (2013a) recommendations include the following (paraphrased):

- Separating the near field from the far field in the PA model so that archaeal data can be used for the near field and bacterial data for the far field,
- PROPMIC values calculated using biosorption data from solutions having a pcH of approximately 8.5 to avoid potential precipitation suspected at higher pcH,
- PROPMIC and CAPMIC values assigned by oxidation state, and
- CAPMIC values based on microbial biomass and sorption capacity.

Based on these recommendations, Reed et al. (2013a) proposed a new set of PROPMIC and CAPMIC values for the element-based approach and a separate set for an oxidation-state-based approach.

5.4.4 Analysis

The analysis of the WIPP microbial colloid model in this report is limited to an analysis of the conservatism included in the Reed et al. (2013a) recommended CAPMIC values (Section 5.4.4.1), and an analysis of the effects of the Reed et al. (2013a) recommendations on baseline concentrations of microbially-associated actinides (Section 5.4.4.2). The development of the Reed et al. (2013a) recommendations is neither described nor evaluated in this report beyond what is discussed in Section 5.4.4.1.

5.4.4.1 Conservatism in Reed et al. (2013a) recommended CAPMIC values

The CAPMIC values recommended in Reed et al. (2013a) are calculated by multiplying microbial actinide concentrations (in units of moles microbial An per cell) by a conservatively high value for the number of cells per liter solution. As explained by Reed et al. (2013a), most halite samples contain no cells, and brine samples from the WIPP underground contain between 10^7 and 10^{10} cell L^{-1} (Francis and Gillow 1994). The concentration used by Reed et al. (2013a) in the calculation of their recommended CAPMIC values is 10^{12} cell L^{-1}, which is two orders of magnitude higher than the maximum value observed by Francis and Gillow (1994) in WIPP brine samples.

5.4.4.2 Effects of Reed et al. (2013a) recommendations on baseline concentrations of microbially-associated actinides

Effects of the Reed et al. (2013a) recommendations on the WIPP microbial colloid model can be evaluated by comparing baseline calculations of microbial actinide concentrations $[\mathrm{AnMIC}]$ for the CRA-2009 implementation to baseline values calculated using the recommended values for PROPMIC and CAPMIC. For each of these calculations, the CRA-2014 baseline dissolved actinide concentration $[\mathrm{An}]$ values are used.

The results for the CRA-2009 PROPMIC and CAPMIC values are displayed in Figure 5-4 and Figure 5-5 (unfilled bars). The microbial actinide concentrations calculated from PROPMIC and baseline $[\mathrm{An}]$ values are far below the CAPMIC value for each actinide species. Only the baseline microbial Pu(III) calculations are within three orders of magnitude of CAPMIC. This implies that the CAPMIC values in the pre-CRA-2014 implementation were never (or rarely) invoked and that the pre-CRA-2014 implementation relied heavily on the PROPMIC and $[\mathrm{An}]$ values to determine $[\mathrm{AnMIC}]$.

Reed et al. (2013a) recommends one set of new PROPMIC and CAPMIC values for archaea and another set for bacteria. These values are further rendered for an oxidation-state-specific and an element-specific

model approach. The archaeal actinide concentrations calculated from baseline $[An]$ and Reed et al. (2013a) recommended archaeal PROPMIC values are compared to the corresponding Reed et al. (2013a) recommended archaeal CAPMIC values in Figure 5-4 (solid bars). The corresponding calculations and parameter values for bacteria are presented in Figure 5-5 (solid bars). The oxidation-specific model set is missing two PROPMIC values and one CAPMIC value (not determined) and is the reason for the three missing values in Figure 5-4.

Compared to the results of the pre-CRA-2014 implementation (unfilled bars), most of the PROPMIC-calculated $[AnMIC]$ values and all of the CAPMIC values are lower in Figure 5-4 (archaea). Many of these the values are much lower. For Am(III), Pu(III), Np(V), and U(VI) the PROPMIC-calculated $[AnMIC]$ values for archaea exceed the archaeal CAPMIC values and therefore final $[AnMIC]$ values would be limited by CAPMIC. Limiting the final archaeal $[AnMIC]$ values to archaeal CAPMIC values where appropriate, most baseline $[AnMIC]$ values calculated using the Reed et al. (2013a) recommended PROPMIC and CAPMIC would be lower than the pre-CRA-2014 implementation. The only actinide species whose baseline microbial colloid concentration would increase due to archaea would be U(IV) by about two orders of magnitude.

Higher PROPMIC-calculated $[AnMIC]$ and CAPMIC values are obtained for the Reed et al. (2013a) recommended values pertaining to bacteria (Figure 5-5). Compared to the CAPMIC values of the CRA-2009 implementation, all of the CAPMIC values are at least two orders of magnitude lower. The PROPMIC-calculated $[AnMIC]$ values, however, may be higher or lower than those calculated in the CRA-2009 implementation. For Am(III), Pu(III), and U(VI), the PROPMIC-calculated $[AnMIC]$ values for bacteria exceed the bacterial CAPMIC values and therefore final $[AnMIC]$ values for bacteria would be limited by CAPMIC. Limiting the final bacterial $[AnMIC]$ values to bacterial CAPMIC values where appropriate, most baseline $[AnMIC]$ values calculated using the Reed et al. (2013a) recommended PROPMIC and CAPMIC would be lower than the CRA-2009 implementation. The only actinide species whose baseline microbial colloid concentration would significantly increase due to bacteria would be Pu(IV) by a factor of 6, Pu(III) in the element-specific approach by a factor of 3, and U(IV) by about three orders of magnitude.

The microbially-bound Am(III) concentrations calculated based on the Reed et al. (2013a) recommendations would be lower by at least two orders of magnitude relative to the CRA-2009 calculations. This result would cause a major reduction in overall WIPP releases because the microbially-bound Am(III) concentration has been a major component of all WIPP releases (e.g., Figure 4-2). This overall reduction would be partially offset by increases in microbial Pu and U(VI) concentrations that would also be predicted to occur due to the Reed et al. (2013a) recommendations.

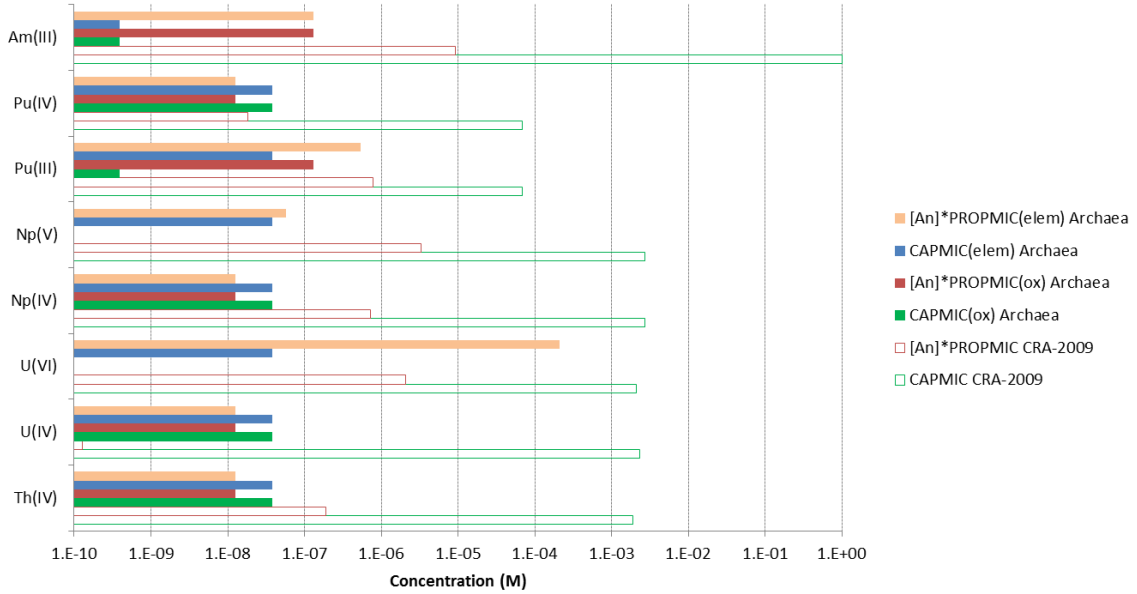

Figure 5-4. Microbial actinide concentrations calculated from baseline CRA-2014 [An] values, Reed et al. (2013a, Table 6-2) oxidation-state-specific (ox) parameters for archaea, and Reed et al. (2013a, Table 6-3) element-specific (elem) parameters for archaea compared to values calculated from CRA-2009 PROPMIC and CAPMIC.

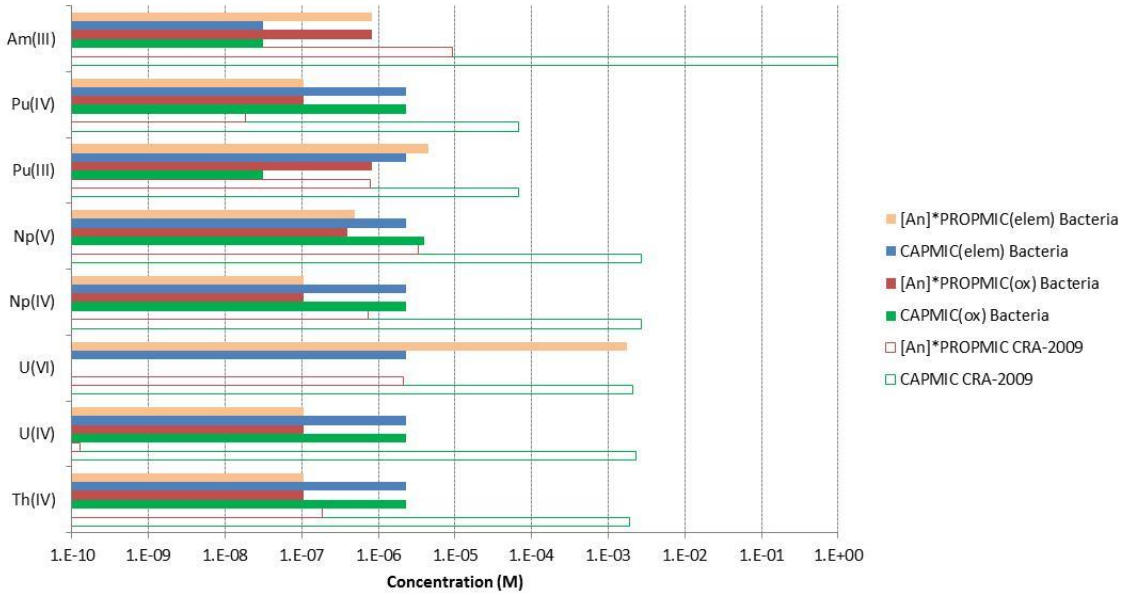

Figure 5-5. Microbial actinide concentrations calculated from baseline CRA-2014 [An] values, Reed et al. (2013a, Table 6-2) oxidation-state-specific (ox) parameters for bacteria, and Reed et al. (2013a, Table 6-3) element-specific (elem) parameters for bacteria compared to values calculated from CRA-2009 PROPMIC and CAPMIC.

5.4.5 Conclusions

5.4.5.1 Changes to the WIPP microbial colloid model proposed by Reed et al. (2013a) are appropriate provided they ensure conservative representation of microbially-bound actinide concentrations.

The recommendations in Reed et al. (2013a) pertaining to the WIPP microbial colloid model are based on data and arguments presented and cited in that report. The recommended values for CAPMIC were set to be conservatively high (Section 5.4.4.1). Whether the recommended values for PROPMIC are sufficiently conservative for the WIPP PA may require further documentation or study because PROPMIC is used exclusively in the calculation of microbial actinide concentrations in the WIPP PA when the product of PROPMIC and $[\mathrm{An}]$ is less than CAPMIC. Due to wide uncertainty distributions for actinide solubility in the WIPP PA (Brush and Domski 2013c), such instances would occur frequently for each actinide species (especially for An(IV) and Np(V) as shown in Section 5.4.4.2) using the Reed et al. (2013a) recommended PROPMIC and CAPMIC values.

6 SUMMARY

In accordance with the Analysis Plan for Evaluating Constraints on Colloid Parameters in the WIPP Repository, AP 152, Rev. 0 (Sassani 2011), an analysis of the WIPP colloid model constraints and parameter values was performed. This work primarily focused on intrinsic colloids, mineral fragment colloids, and humic substance colloids, with a lesser focus on microbial colloids. Comments by the EPA concerning intrinsic Th(IV) colloids and Mg-Cl-OH mineral fragment colloids were addressed, assumptions and data used to constrain colloid model calculations were evaluated, and inconsistencies found between data and model parameter values were identified. This work resulted in the specific conclusions listed below. These conclusions are developed and discussed in the body of the report. All calculations in this report are stored on the VMS (Virtual Memory System) in LIBAP152_FILES class AP152.

Mineral fragment colloids

- The value of CONCMIN should not be increased to account for potential Mg-Cl-OH colloids.
- The value of CONCMIN for each actinide element could justifiably be reduced, but doing so would have little effect on WIPP releases.
- The predominant phases of Pu (sorbed and/or mineral) associated with colloids in Pu-iron interaction studies should be investigated.

Intrinsic colloids

- A non-zero CONCINT value for Th(IV) intrinsic colloids should be used in the WIPP PA.
- The set of solubility data used to determine dissolved concentration distributions for the WIPP PA model should exclude solubility measurements known or likely to contain large contributions from intrinsic colloids.
- CONCINT values should be used for each actinide species that forms significant concentrations of intrinsic colloids in WIPP brines.

Humic colloids

- The stability of humic and fulvic acids in WIPP brines in the presence of MgO and inorganic colloids requires further laboratory study.
- If humic substances are found to be stable at potentially significant concentrations in WIPP brines in the presence of MgO, laboratory studies will be needed to directly measure the association of An(III) and An(IV) actinides with humic colloids under these same conditions.
- To be consistent with the methodology developed for the CCA, PHUMSIM and PHUMCIM for U(VI) should be calculated using the log $\beta_{1:An}$ values of Labonne-Wall et al. (1999) and the established dissolved U(VI) concentration of 10^{-3} M.

Microbial colloids

- Changes to the WIPP microbial colloid model proposed by Reed et al. (2013a) are appropriate provided they ensure conservative representation of microbially-bound actinide concentrations.

7 REFERENCES

Abdel-Fattah, A. I., D. Zhou, H. Boukhalfa, S. Tarimala, D. Ware, and A. A. Keller 2013. "Dispersion stability and electrokinetic properties of intrinsic plutonium colloids: Implications for subsurface transport." *Environmental Science & Technology*. 47:5626-5634.

Alexander, W. R., J. A. Berry, M. J. Kelly, and S. W. Swanton 2011. *Review of colloids in the geosphere and their treatment in performance assessments.* NPO003512. Report to NDA-RWMD. Serco Ltd., Oxfordshire, UK.

Altmaier, M., V. Neck, and T. Fanghanel 2008. "Solubility of Zr(IV), Th(IV) and Pu(IV) hydrous oxides in CaCl(2) solutions and the formation of ternary Ca-M(IV)-OH complexes." *Radiochimica Acta*. 96(9-11):541-550.

Altmaier, M., V. Neck, and T. Fanghänel 2004. "Solubility and colloid formation of Th(IV) in concentrated NaCl and MgCl2 solution." *Radiochimica Acta*. 92:537-543.

Ams, D. A., J. S. Swanson, J. E. S. Szymanowski, J. B. Fein, M. Richmann, and D. T. Reed 2013. "The effect of high ionic strength on neptunium (V) adsorption to a halophilic bacterium." *Geochimica Et Cosmochimica Acta*. 110:45-57.

Baskaran, M., P. H. Santschi, G. Benoit, and B. D. Honeyman 1992. "Scavenging of thorium isotopes by colloids in seawater of the Gulf of Mexico." *Geochimica et Cosmochimica Acta*. 56(9):3375-3388.

Bitea, C., C. Walther, J. I. Kim, H. Geckeis, T. Rabung, F. J. Scherbaum, and D. G. Cacuci 2003. "Time-resolved observation of ZrO2-colloid agglomeration." *Colloids and Surfaces A: Physicochem. Eng. Aspects*. 215:55-66.

Borgnino, L. 2013. "Experimental determination of the colloidal stability of Fe(III)-montmorillonite: Effects of organic matter, ionic strength and pH conditions." *Colloids and Surfaces a-Physicochemical and Engineering Aspects*. 423:178-187.

Borkowski, M., M. Richmann, J. F. Lucchini, and D. T. Reed 2012. *Solubility of An(IV) in WIPP Brine: Thorium Analog Studies in WIPP Simulated Brine*. LCO-ACP-17. Los Alamos National Laboratory, Los Alamos, New Mexico.

Brush, L. H. 1990. *Test Plan for Laboratory and Modeling Studies of repository and Radionuclide Chemistry for the Waste Isolation Pilot Plant*. SAND90-0266. Sandia National Laboratories, Albuquerque, New Mexico.

Brush, L. H. 1995. *Systems Priority Method – Iteration 2 Baseline Position Paper: Gas Generation in the Waste Isolation Pilot Plant*. Sandia National Laboratories, Albuquerque, New Mexico.

Brush, L. H., and P. S. Domski 2013a. *Geochemical process modeling for the Waste Isolation Pilot Plant (WIPP) 2014 Compliance Recertification Application (CRA-2014) Performance Assessment (PA) Calculations*. Technical Abstracts of the ABC Salt III Workshop, April 15-17, 2013, Sante Fe, New Mexico.

Brush, L. H., and P. S. Domski 2013b. *Prediction of Baseline Actinide Solubilities for the WIPP CRA-2014 PA*. Sandia National Laboratories, Carlsbad, New Mexico.

Brush, L. H., and P. S. Domski 2013c. *Uncertainty Analysis of Actinide Solubilities for the WIPP CRA-2014 PA*. Analysis report, February 22, 2013. Sandia National Laboratories, Carlsbad, New Mexico.

Buck, E., and D. C. Sassani 2007. *Waste Form and In-Drift Colloids-Associated Radionuclide Concentrations: Abstraction and Summary*. Sandia National Laboratories, Albuquerque, New Mexico.

Butcher, B. M. 1990. *Preliminary Evaluation of Potential Engineered Modifications for the Waste Isolation Pilot Plant (WIPP)*. SAND89-3095. Sandia National Laboratories, Albuquerque, New Mexico.

Derjaguin, B. V., and L. Landau 1941. "Theory of stability of strongly charged lyophobic sols and of the adhesion of strongly charged particles in solutions of electrolytes." *Acta Physicochim*. 17:633-662.

DOE 1996. *Title 40 CFR Part 191 Compliance Certification Application for the Waste Isolation Pilot Plant*. DOE/CAO-1994-2184. U.S. Department of Energy, Carlsbad, NM.

DOE 2004. *Title 40 CFR 191 Parts B and C Compliance Recertification Application for the Waste Isolation Pilot Plant, 10 vols*. DOE/WIPP 2004-3231. U.S. Department of Energy Carlsbad Field Office, Carlsbad, New Mexico.

DOE 2009. *Title 40 CFR Part 191 Subparts B and C Compliance Recertification Application for the Waste Isolation Pilot Plant*. DOE/WIPP 09 3424. U.S. Department of Energy Carlsbad, NM.

EPA 2010. *Technical Support Document for Section 194.24: Evaluation of the Compliance Recertification Actinide Source Term, Backfill Efficacy and Culebra Dolomite Distribution Coefficient Values (Revision 1)*. Docket No. A-98-49, Item II-B1-25. EDOCKET NO: EPA-HQ-OAR-2009-0330. U.S. Environmental Protection Agency.

Francis, A. J., and J. B. Gillow 1994. *Effects of microbial processes on gas generation under expected Waste Isolation Pilot Plant repository conditions*. SAND93-7036. Sandia National Laboratories, Albuquerque, New Mexico.

Gillow, J. B., A. J. Francis, C. J. Dodge, R. Harris, T. J. Beveridge, P. V. Brady, and H. W. Papenguth 1998. *Actinide biocolloid formation in brine by halophilic bacteria*. 22nd Symposium on Scientific Basis for Nuclear Waste Management held at the 1998 MRS Fall Meeting, Boston, MA, Nov. 30 - Dec 4, 1998.

Gruber, C., A. Legat, M. Pfaffenhuemer, C. Radax, G. Weidler, H. J. Busse, and H. Stan-Lotter 2004. "Halobacterium noricense sp nov., an archaeal isolate from a bore core of an alpine Permian salt deposit, classification of Halobacterium sp NRC-1 as a strain of H-salinarum and emended description of H-salinarum." *Extremophiles*. 8(6):431-439.

Helton, J. C., J. E. Bean, J. W. Berglund, F. J. Davis, K. Ecomony, J. W. Garner, J. D. Johnson, R. J. MacKinnon, R. J. Miller, D. G. O'Brien, J. L. Ramsey, J. D. Schreiber, A. Shinta, L. N. Smith, D. M. Stoelzel, C. Stockman, and P. Vaughn 1998. *Uncertainty and Sensitivity Analysis Results Obtained in the 1996 Performance Assessment for the Waste Isolation Pilot Plant*. SAND98-0365. Sandia National Laboratories.

Hu, J. D., Y. Zevi, X. M. Kou, J. Xiao, X. J. Wang, and Y. Jin 2010. "Effect of dissolved organic matter on the stability of magnetite nanoparticles under different pH and ionic strength conditions." *Science of the Total Environment*. 408(16):3477-3489.

Johnson, G. L., and L. M. Toth 1978. *Plutonium(IV) and thorium(IV) hydrous polymer chemistry*. ORNL/TM-6365. Oak Ridge National Laboratory, Oak Ridge, Tennessee.

Kelly, T. 2010. *Untitled letter with enclosure to D.C Moody with fourth set of CRA comments and requests for additional information, February 22, 2010*. U.S. Environmental Protection Agency, Washington, DC.

Kim, J. I. 1992. "Actinide colloid generation in groundwater." *Radiochimica Acta*. 52/53(pt. 1):71-81.

Kim, J. I. 1994. "Actinide colloids in natural aquifer systems." *MRS Bulletin*. 19(12):47-53.

Kim, J. L., and T. Sekine 1991. "Complexation of neptunium(V) with humic acid." *Radiochimica Acta*. 55(4):187-192.

Labonne-Wall, N., G. R. Choppin, C. Lopez, and J.-M. Monsallier 1999. *Interaction of uranyl with humic and fulvic acids at high ionic strength*. Actinide Speciation in High Ionic Strength Media, edited by Reed, D.T., Clark, S.B., and Linfeng Rao. Plenum Publishers, New York.

LANL 2010. *Reduction of Higher-Valent Plutonium by Iron under WIPP-Relevant Conditions: Data Summary and Recommendations*. LCO-ACP-09, Rev. 0. Los Alamos National Laboratory, Los Alamos, New Mexico.

Laszak, I., and G. R. Choppin 2001. "Interaction study between Ca2+ and humic acids in brine media." *Radiochimica Acta*. 89(10):653-659.

McGenity, T. J., R. T. Gemmell, W. D. Grant, and H. Stan-Lotter 2000. "Origins of halophilic microorganisms in ancient salt deposits." *Environmental Microbiology*. 2(3):243-250.

Moser, C., R. Kautenburger, and H. Philipp Beck 2012. "Complexation of europium and uranium by humic acids analyzed by capillary electrophoresis-inductively coupled plasma mass spectrometry." *Electrophoresis*. 33(9-10):1482-1487.

Neck, V., M. Altmaier, R. Muller, A. Bauer, T. Fanghanel, and J. I. Kim 2003. "Solubility of crystalline thorium dioxide." *Radiochimica Acta*. 91(5):253-262.

Neck, V., and J. I. Kim 2001. "Solubility and hydrolysis of tetravalent actinides." *Radiochimica Acta*. 89:1-16.

Neck, V., R. Muller, M. Bouby, M. Altmaier, J. Rothe, M. A. Denecke, and J. I. Kim 2002. "Solubility of amorphous Th(IV) hydroxide - application of LIBD to determine the solubility product and EXAFS for aqueous speciation." *Radiochimica Acta*. 90(9-11):485-494.

Nitsche, H., K. Roberts, R. C. Gatti, T. Prussin, K. Becraft, S. C. Leung, S. A. Carpenter, and C. F. Novak 1992. *Plutonium Solubility and Speciation Studies in a Simulant of Air Intake Shaft Water from the Culebra Dolomite at the Waste Isolation Pilot Plant*. SAND92-0659. Sandia National Laboratories, Albuquerque, NM.

Nitsche, H., K. Roberts, R. Xi, T. Prussin, K. Becraft, I. Al Mahamid, H. B. Silber, S. A. Carpenter, R. C. Gatti, and C. F. Novak 1994. *Long Term Plutonium Solubility and Speciation Studies in a Synthetic Brine*. Radiochimica Acta, Special Issue: Chemistry and Migration Behaviour of Actinides and Fission Products in the Geosphere, Proceedings of the Fourth International Conference, Charleston, SC, December 12-17, 1993. Munich: R. Oldenbourg Verlag. Vol. 66/67, 3-8.

Palomino, D., and S. Stoll 2013. "Fulvic acids concentration and pH influence on the stability of hematite nanoparticles in aquatic systems." *Journal of Nanoparticle Research*. 15(2).

Papenguth, H. W. 1996. *H.W. Papenguth to Christine T. Stockman: " Parameter Record Package for Colloidal Actinide Source Term Parameters" May 7, 1996: Attachment A: Rationale for Definition of Paramter Values for Humic Substances"*.

Powell, B. A., Z. R. Dai, M. Zavarin, P. H. Zhao, and A. B. Kersting 2011. "Stabilization of Plutonium Nano-Colloids by Epitaxial Distortion on Mineral Surfaces." *Environmental Science & Technology*. 45(7):2698-2703.

Rand, M. H., F. J. Mompean, J. Perrone, and M. Illemass*ne 2008. *Chemical thermodynamics of thorium*. Chemical thermodynamics. OECD Pub., Paris, France.

Reed, D., J. Swanson, J. F. Lucchini, and M. Richmann 2013a. *Intrinsic, mineral and microbial colloid enhancement parameters for the WIPP actinide source term*. LANL-CO ACRSP/LCO-ACP-18. Los Alamos National Laboratory, Los Alamos, NM.

Reed, D. T., J. F. Lucchini, M. K. Richmann, and M. Borkowski 2013b. *Long-term plutonium speciation in Fe-dominated high ionic-strength brines*. Technical Abstracts of the ABC Salt III Workshop, April 15-17, 2013, Santa Fe, New Mexico.

Reiller, P. E., N. D. M. Evans, and G. Szabo 2008. "Complexation parameters for the actinides(IV)-humic acid system: a search for consistency and application to laboratory and field observations." *Radiochimica Acta*. 96(6):345-358.

Roselle, G. T. 2013a. *Anoxic corrosion of steel and lead in Na-Cl(+/-)Mg dominated brine*. Technical Abstracts of the ABC Salt III Workshop, April 15-17, 2013, Santa Fe, New Mexico.

Roselle, G. T. 2013b. *Summary of colloid parameters to be implemented in the CRA-2014 PA*. Letter from G. Roselle to S. Dunagan, February 15, 2013. Sandia National Laboratories, Carlsbad, New Mexico.

Sakuragi, T., S. Sawa, S. Sato, T. Kozaki, T. Mitsugashira, M. Hara, and Y. Suzuki 2005. "Interaction of americium(III) with humic acid over wide pH region." *Journal of Radioanalytical and Nuclear Chemistry*. 265(3):349-353.

Sassani, D. C. 2011. *Analysis Plan for Evaluating Constraints on Colloid Parameters in the WIPP Repository*. AP-152. Sandia National Laboratories, Albuquerque, New Mexico.

Shi, H., M. Chu, and P. Zhang 2010. "Optical properties of UO2 and PuO2." *Journal of Nuclear Materials*. 400:151-156.

Swanson, J. S., D. M. Norden, H. M. Khaing, and D. T. Reed 2013. "Degradation of Organic Complexing Agents by Halophilic Microorganisms in Brines." *Geomicrobiology Journal*. 30(3):189-198.

Swanson, J. S., D. T. Reed, D. A. Ams, D. M. Norden, and K. A. Simmons 2012. *Status report on the microbial characterization of halite and groundwater samples from the WIPP*. LANL/ACRSP Report LCO-ACP-12, LA-UR 12-22824. Los Alamos National Laboratory, Los Alamos, New Mexico.

Swanson, J. S., and K. Simmons 2013. *Update on microbial characterization of WIPP groundwaters*. LANL/ACRSP report LCO-ACP-20, LA-UR 13-20623. Los Alamos National Laboratory, Los Alamos, New Mexico.

Telander, M. R., and R. E. Westerman 1997. *Hydrogen Generation by Metal Corrosion in Simulated Waste Isolation Pilot Plant Environments*. SAND96-2538. Sandia National Laboratories, Albuquerque, New Mexico.

Tierney, M. 1996. *WIPP Data Entry Form 464, Id: 3429, Idmtrl: PHUMOX3, Idpram: PHUMCIM*. Sandia National Laboratories, Carlsbad, New Mexico.

Traexler, K. A., S. Utsunomiya, A. B. Kersting, and R. C. Ewing 2004. *Colloid transport of radionuclides: Yucca Mountain performance assessment*. Scientific Basis for Nuclear Waste Management XXVII, Symposium held April 12-16, 2004, San Francisco, CA, USA. 807, 1-6. Materials Research Society, Warrendale, Pennsylvania.

Vandenborre, J., A. Abdelouas, and B. Grambow 2008. "Discrepancies in thorium oxide solubility values: a new experimental approach to improve understanding of oxide surface at solid/solution interface." *Radiochimica Acta*. 96(9-11):515-520.

Verwey, E. J. W., and J. T. G. Overbeek 1948. *Theory of the stability of lyophobic colloids*. Elsevier, Amsterdam.

Wall, N. A., M. Borkowski, J. F. Chen, and G. R. Choppin 2002. "Complexation of americium with humic, fulvic and citric acids at high ionic strength." *Radiochimica Acta*. 90(9-11):563-568.

Wall, N. A., and G. R. Choppin 2003. "Humic acids coagulation: influence of divalent cations." *Applied Geochemistry*. 18(10):1573-1582.

Wall, N. A., and S. A. Mathews 2003. *Humic acids in the WIPP*. Presentation at the 2003 Radiochemistry Conference, July 14-16, 2003. Sandia National Laboratories, Carlsbad, New Mexico.

Wall, N. A., and S. A. Mathews 2005. "Sustainability of humic acids in the presence of magnesium oxide." *Applied Geochemistry*. 20:1704-1713.

Wang, Y., and L. H. Brush 1996. *Estimates of gas-generation parameters for the long-term WIPP performance assessment*. Memo to Martin S. Tierney, January 26, 1996. ERMS 231943. Sandia National Laboratories, Carlsbad, New Mexico.

Xiong, Y.-L., L. H. Brush, J. W. Garner, and J. J. Long 2010a. *Responses to three EPA comments pertaining to comparisons of measured and predicted dissolved and colloidal Th(IV) and Am(III) concentrations*. Analysis report, May 4, 2010. Sandia National Laboratories, Carlsbad, NM.

Xiong, Y.-L., H. Deng, M. Nemer, and S. Johnson 2010b. "Experimental Determination of the Solubility Constant for Magnesium Chloride Hydroxide Hydrate (Mg3Cl(OH)5•4H2O, Phase 5) at Room Temperature, and Its Importance to Nuclear Waste Isolation in Geological Repositories in Salt Formations." *Geochimica et Cosmochimica Acta*. 74:4605-4611.

Xiong, Y.-L., and A. C. S. Lord 2008. "Experimental investigations of the reaction path in the MgO–CO2–H2O system in solutions with ionic strengths, and their applications to nuclear waste isolation." *Applied Geochemistry*. 23:1634–1659.

Xiong, Y. L., L. H. Brush, P. S. Domski, and J. J. Long 2011. *Uncertainty Analysis of Actinide Solubilities for the WIPP CRA-2009 PABC, Rev. 1*. Analysis report, January 24, 2011. Sandia National Laboratories, Carlsbad, New Mexico.

Zhao, P., and S. A. Steward 1997. *Literature review of intrinsic actinide colloids related to spent fuel waste package release rates*. UCRL-ID-126039. Lawrence Livermore National Laboratory, Livermore, California.

DISTRIBUTION

1	MS0747	David C. Sassani	Org. 6222
1	MS0747	Paul E. Mariner	Org. 6224
1	MS0899	Technical Library	9536 (electronic copy)

Sandia National Laboratories